QUARTERLY OF APPLIED MATHEMATICS
VOLUME , NUMBER 0
XXXX XXXX, PAGES 000–000
S 0033-569X(XX)0000-0

LEFT-INVARIANT PARABOLIC EVOLUTIONS ON $SE(2)$ AND CONTOUR ENHANCEMENT VIA INVERTIBLE ORIENTATION SCORES

PART II: NONLINEAR LEFT-INVARIANT DIFFUSIONS ON INVERTIBLE ORIENTATION SCORES

By

REMCO DUITS (*Department of Mathematics/Computer Science and Department of Biomedical Engineering, Eindhoven University of Technology, Den Dolech 2, P.O. Box 513, 5600MB Eindhoven, The Netherlands.*)

AND

ERIK FRANKEN (*Department of Biomedical Engineering, Eindhoven University of Technology, Den Dolech 2, P.O. Box 513, 5600MB Eindhoven, The Netherlands.*)

Abstract. By means of a special type of wavelet unitary transform we construct an orientation score from a grey-value image. This orientation score is a complex-valued function on the 2D-Euclidean motion group $SE(2)$ and gives us explicit information on the presence of local orientations in an image. As the transform between image and orientation score is unitary we can relate operators on images to operators on orientation scores in a robust manner. In this part we consider nonlinear adaptive diffusion equations on these invertible orientation scores. These nonlinear diffusion equations lead to clear improvements of the celebrated standard "coherence enhancing diffusion"-equations on images as they can cope with crossing contours. Here we employ differential geometry on $SE(2)$ to align the diffusion with optimized local coordinate systems attached to an orientation score, allowing us to include local features such as adaptive curvature in our diffusions.

Received November 12, 2008and in revised form ??
2000 *Mathematics Subject Classification.* Primary 58J65 ; 49Q20; 22E30 ; Secondary 34B30, 37L05, 47D06 .
Key words and phrases. Nonlinear Diffusion Equations on Lie groups, Cartan Connection, Fiber bundles, Image Analysis, Coherence Enhancing Diffusion .
The Netherlands Organization for Scientific Research is gratefully acknowledged for financial support.
Current address: Department of Mathematics/Computer Science and Department of Biomedical Engineering, Eindhoven University of Technology, Den Dolech 2, P.O. Box 513, 5600MB Eindhoven, The Netherlands.
E-mail address: R.Duits@tue.nl
E-mail address: E.M.Franken@tue.nl

1. Introduction. In many noisy medical images elongated structures occur that cross each other. Therefor in the previous part we proposed to enhance these elongated structures using *linear* diffusions on the Euclidean motion group $SE(2)$. In this part we go one step further and consider non-linear diffusion on $SE(2)$. The advantage of the non-linear approach is that we can adapt the diffusion process depending on the orientation confidence of local elongated structures. Just like in the previous part we will process the image via diffusions on invertible orientation scores, which we will briefly explain next.

Image analysis usually starts with the sampling of a square integrable grey-value image $f : \mathbb{R}^2 \to \mathbb{R}$ by a function $\psi \in \mathbb{L}_2(\mathbb{R}^2) \cap \mathbb{L}_1(\mathbb{R}^2)$ via $f \mapsto (\psi, f)_{\mathbb{L}_2(\mathbb{R}^2)}$. To probe an image at every location $\mathbf{x} \in \mathbb{R}^2$ and in every direction $e^{i\theta} \in \mathbb{T}$ one translates and rotates an anisotropic wavelet ψ by means of a representation $g \mapsto \mathcal{U}_g$ of the 2D-Euclidean motion group $SE(2)$ given by

$$\mathcal{U}_g\psi(\mathbf{y}) = \psi(R_\theta^{-1}(\mathbf{y}-\mathbf{x})),\ g = (\mathbf{x}, e^{i\theta}) \in SE(2). \tag{1.1}$$

The result of such an image sampling is a function $\mathcal{W}_\psi f : SE(2) \to \mathbb{C}$ on the Euclidean motion group manifold $SE(2) = \mathbb{R}^2 \rtimes \mathbb{T}$, which is given by

$$\mathcal{W}_\psi f(g) = (\mathcal{U}_g\psi, f)_{\mathbb{L}_2(\mathbb{R}^2)} = \int_{\mathbb{R}^2} \overline{\psi(R_\theta^{-1}(\mathbf{y}-\mathbf{x}))} f(\mathbf{y})\, \mathrm{d}\mathbf{y},\ \text{with } g = (\mathbf{x}, e^{i\theta}), \tag{1.2}$$

and where $R_\theta = \begin{pmatrix} \cos\theta & -\sin\theta \\ \sin\theta & \cos\theta \end{pmatrix} \in \mathrm{SO}(2)$. Throughout this article we refer to this function $(\mathbf{x}, e^{i\theta}) \mapsto \mathcal{W}_\psi f(\mathbf{x}, e^{i\theta})$ as the *orientation score* $\mathcal{W}_\psi f$ of grey-value image f.

As we have shown in [14], [12, ch:4.4, App.7.2] the transformation $\mathcal{W}_\psi$ is a unitary linear operator from $\mathbb{L}_2(\mathbb{R}^2)$ onto the unique reproducing kernel space $\mathbb{C}_K^{SE(2)}$ consisting of complex-valued functions on $SE(2)$ with reproducing kernel

$$K(g,h) = (\mathcal{U}_g\psi, \mathcal{U}_h\psi)_{\mathbb{L}_2(\mathbb{R}^2)}. \tag{1.3}$$

The generation of orientation scores and the reconstruction of images thereof has been the subject of previous publications, [12, 13, 15, 27] and in part I [18], we have derived the essential equality in Fourier domain (of the spatial part only):

$$\|\mathcal{W}_\psi f\|^2_{\mathbb{C}_K^{SE(2)}} = \int_{\mathbb{R}^2}\int_{\mathbb{T}} |(\mathcal{F}\mathcal{W}_\psi f)(\boldsymbol{\omega}, e^{i\theta})|^2 \mathrm{d}\theta\, \frac{1}{M_\psi(\boldsymbol{\omega})}\, \mathrm{d}\boldsymbol{\omega} = \|f\|^2_{\mathbb{L}_2(\mathbb{R}^2)}, \tag{1.4}$$

where $M_\psi(\boldsymbol{\omega}) := \int_0^{2\pi} |\mathcal{F}\psi(R_\theta^T\boldsymbol{\omega})|^2 \mathrm{d}\theta$ and where we assume that ψ is chosen such that $M_\psi > 0$, so that $\frac{1}{M_\psi}$ is well-defined. Here $\mathcal{F}$ denotes the usual unitary Fourier transform on $\mathbb{L}_2(\mathbb{R}^2)$ given by $\mathcal{F}\psi(\boldsymbol{\omega}) = \frac{1}{2\pi}\int_{\mathbb{R}^2} \psi(\mathbf{x}) e^{-i\mathbf{x}\cdot\boldsymbol{\omega}} \mathrm{d}\mathbf{x}$.

From (1.4) we obtain the reconstruction formula

$$f \quad = \mathcal{W}_\psi^*\mathcal{W}_\psi[f] = \mathcal{F}^{-1}\left[\boldsymbol{\omega} \mapsto \int_0^{2\pi} \mathcal{F}[\mathcal{W}_\psi f(\cdot, e^{i\theta})](\boldsymbol{\omega})\ \mathcal{F}[\mathcal{R}_{e^{i\theta}}\psi](\boldsymbol{\omega})\, \mathrm{d}\theta\ M_\psi^{-1}(\boldsymbol{\omega})\right]. \tag{1.5}$$

The transformation between images and orientation scores preserves the $\mathbb{L}_2$-norm iff

$$\|f\|^2_{\mathbb{L}_2(\mathbb{R}^2)} = \|\mathcal{W}_\psi f\|^2_{\mathbb{L}_2(SE(2))} \Leftrightarrow M_\psi = 1. \tag{1.6}$$

It can be shown that for kernels $\psi \in \mathbb{L}_2(\mathbb{R}^2) \cap \mathbb{L}_1(\mathbb{R}^2)$ the function M_ψ is a continuous function vanishing at infinity. So for such kernels the wavelet transform $\mathcal{W}_\psi$ can not be an isometry from $\mathbb{L}_2(\mathbb{R}^2)$ into $\mathbb{L}_2(SE(2))$.

$$
\begin{tikzcd}
\boxed{\begin{array}{c}\textbf{Image}\\ f \in \mathbb{L}_2(\mathbb{R}^2)\end{array}} \arrow[r, "\mathcal{W}_\psi"] \arrow[d, "\Upsilon"'] & \boxed{\begin{array}{c}\textbf{Orientation Score}\\ U_f \in \mathbb{C}_K^{SE(2)} \subset \mathbb{L}_2(SE(2))\end{array}} \arrow[d, "\Phi"] \\
\boxed{\begin{array}{c}\textbf{Processed Image}\\ \Upsilon[f] = \mathcal{W}_\psi^*[\Phi[U_f]]\end{array}} & \boxed{\begin{array}{c}\textbf{Processed Score}\\ \Phi[U_f] \in \mathbb{L}_2(SE(2))\end{array}} \arrow[l, "(\mathcal{W}_\psi^*)^{\mathrm{ext}} = \mathcal{W}_\psi^* \mathbb{P}_\psi"]
\end{tikzcd}
$$

FIG. 1. Top Row: The complete scheme; for proper anisotropic wavelets ψ the linear map $\mathcal{W}_\psi$ is unitary from $\mathbb{L}_2(\mathbb{R}^2)$ onto the closed subspace $\mathbb{C}_K^{SE(2)}$ of orientation scores. We can uniquely relate a transformation $\mathbb{P}_\psi \circ \Phi : \mathbb{C}_K^{SE(2)} \to \mathbb{C}_K^{SE(2)}$ on an orientation score to a transformation on an image $\Upsilon_\psi = (\mathcal{W}_\psi^*) \circ \mathbb{P}_\psi \circ \Phi \circ \mathcal{W}_\psi$, Here $\mathbb{P}_\psi$ denotes the orthogonal projection onto $\mathbb{C}_K^{SE(2)}$ given by $\mathbb{P}_\psi U(g) = \int_{SE(2)} K(g,h)U(h)\,\mathrm{d}h$, using reproducing kernel (1.3).

This problem can be tackled by choosing ψ, within the dual space $\mathbb{H}^{-k,2}(\mathbb{R}^2)$ of the k-th order, $k > 1$, isotropic Sobolev space $\mathbb{H}^{k,2}(\mathbb{R}^n)$ such that $M_\psi = 1$. Since then the associated distributional transform $\mathfrak{W}_\Psi : \mathbb{H}^{k,2}(\mathbb{R}^2) \to \mathbb{C}_K^{SE(2)}$ defined by $\mathfrak{W}_\Psi f(\mathbf{x}, e^{i\theta}) = \langle \Psi, \mathcal{U}_{(\mathbf{x},e^{i\theta})^{-1}} f\rangle$, for all $f \in H^k(\mathbb{R}^2)$, extends to an isometry from $\mathbb{L}_2(\mathbb{R}^2)$ into $\mathbb{L}_2(SE(2))$.

Alternatively, one may restrict the transform $\mathcal{W}_\psi$ to the space of images $f \in \mathbb{L}_2^{\varrho}(\mathbb{R}^2)$ whose Fourier transform has support within a given disc with radius $\varrho > 0$ as motivated in Part I. If we now choose $\psi \in \mathbb{L}_2^{\varrho}(\mathbb{R}^2)$ such that $M_\psi = 1_{B_{\mathbf{0},\varrho}}$, where $B_{\mathbf{0},\varrho} = \{\boldsymbol{\omega} \in \mathbb{R}^2 \mid \|\boldsymbol{\omega}\| < \rho\}$then the unitary operator $\mathcal{W}_\psi : \mathbb{L}_2^{\varrho}(\mathbb{R}^2) \to \mathbb{C}_K^{SE(2)}$ between the space of "disc-limited" images and the space of orientation scores preserves the $\mathbb{L}_2$-norm.

These two approaches lead to two different classes of proper wavelets, as explained in [13, ch: 4.3 and ch: 4.4], [12]. In both approaches the engineering rationale behind $M_\psi = 1$ is that the auto-correlations of all rotated kernels $\mathcal{R}_{e^{i\theta}}\psi$ together fill op the Fourier-spectrum. Note that $M_\psi(\boldsymbol{\omega}) = \mathcal{F}(\int_0^{2\pi} \mathcal{R}_{e^{i\theta}}\psi * \mathcal{R}_{e^{i\theta}}\overline{\check{\psi}}\,\mathrm{d}\theta)(\boldsymbol{\omega})$, with $\overline{\check{\psi}}(\mathbf{x}) = \overline{\psi(-\mathbf{x})}$.

As a result for appropriate choice of ψ (say $M_\psi = 1$) a small perturbation on an image f corresponds to a small perturbation on its orientation score $\mathcal{W}_\psi f$ and vice versa and consequently operators Φ on the space of orientation scores are bijectively related to operators on images Υ_ψ in a stable manner by

$$\Upsilon_\psi \leftrightarrow \Phi \;\Leftrightarrow\; \Upsilon_\psi = \mathcal{W}_\psi^* \circ \Phi \circ \mathcal{W}_\psi, \tag{1.7}$$

see Figure 1. This bijection is manifest if Φ maps the space of orientation scores $\mathbb{C}_K^{SE(2)}$ into itself. With the operators Φ we consider in this article this is usually not the case. Recall from part I [18] that this does not cause any problems if we naturally extend the adjoint, recall [18, eq. 4.4], to the space $\mathbb{L}_2(SE(2))$. However one should keep in mind that the effective operator from the space of orientation scores into itself is given by $\mathbb{P}_\psi \circ \Phi$, see Figure 1. Furthermore, in part I we have explained that Φ must be a nonlinear left-invariant operator. Therefor we considered collision distributions obtained from a forward linear diffusion resolvent and a backward linear diffusion resolvent, that is in part I [18, eq. 4.1 and 4.2] and [16], [14], [13], we considered the case where operator $\Phi : \mathbb{C}_K^{SE(2)} \to \mathbb{L}_2(SE(2))$ is given by $\Phi(\mathcal{W}_\psi f) = (Q^{D,\mathbf{a}}(\underline{A}) - \alpha I)^{-1}(\chi(\Re\{\mathcal{W}_\psi f\}))$ $\cdot$

$((Q^{D,\mathbf{a}}(\underline{A}))^* - \alpha I) - 1(\chi(\Re\{\mathcal{W}_\psi f\}))$, where we recall the quadratic form $Q^{D,\mathbf{a}}(\underline{A})$ on the left-invariant vector fields on $SE(2)$:

$$\begin{array}{l} \underline{\mathcal{A}} := \{\mathcal{A}_1, \mathcal{A}_2, \mathcal{A}_3\} = \{\partial_\theta, \partial_\xi, \partial_\eta\}, \qquad \xi = x\cos\theta + y\sin\theta, \eta = -x\sin\theta + y\cos\theta, \\ Q^{\mathbf{D},\mathbf{a}}(\underline{\mathcal{A}}) = \sum_{i=1}^{3}\left(-a_i\mathcal{A}_i + \sum_{j=1}^{3}\mathcal{A}_i D_{ij}\mathcal{A}_j\right),\ a_i, D_{ij} \in \mathbb{R}, D^T = D \geq 0. \end{array} \tag{1.8}$$

with $\mathbf{a} = (a_1, a_2, a_3) \in \mathbb{R}^3$, $D = [D_{ij}] \in \mathbb{R}^{3\times 3}$. Here we recall that χ was some monotonic grey-value transformation to put a soft threshold on weak responses in the orientation score. Although the linear parts of these operators, such as

$$\left(((Q^{D,\mathbf{a}}(\underline{A}))^* - \alpha I)^{-1}U\right)(g) = \left(\int_0^\infty K_s^{D,-\mathbf{a}} e^{-\alpha s} \mathrm{d}s *_{SE(2)} U\right)(g) = (R_\alpha^{D,-\mathbf{a}} *_{SE(2)} U)(g).$$

are easily computed by means of $SE(2)$-convolution with the corresponding Green's functions $R_\alpha^{D,-\mathbf{a}}$ which we derived explicitly in part I and [16], they suffer from the practical drawback that the involved convolution kernels $R_\alpha^{D,-\mathbf{a}}$, $R_\alpha^{D,\mathbf{a}}$ take care of *constant* diffusion and convection. Here it is possible (by suitable choice of $\mathbf{a}$ and D) to incorporate curvature into contour completion and enhancement, as first reported (for contour completion) by August & Zucker [5].

In this part we go one step further, we propose $\Phi_t : \mathbb{C}_K^{SE(2)} \to \mathbb{L}_2(SE(2))$ as *nonlinear adaptive* diffusion equations on *invertible* orientation scores, with stopping time $t > 0$. Here we will not consider products of linear resolvent equations, but we will consider nonlinear evolutions, without convection, given by

$$\left\{ \begin{array}{l} \partial_t U(g,t) = Q^{D(U),\mathbf{a}=\mathbf{0}}\, U(g,t), \qquad g \in SE(2), t > 0 \\ U(g,0) = \mathcal{W}_\psi f(g), \qquad g \in SE(2), \end{array} \right. \tag{1.9}$$

where conductivity $D(U)$ depends on (the local differential structure of) $(g,t) \mapsto U(g,t)$.

Here we use locally optimal exponential curve fits to the absolute value of an orientation score. These optimal exponential curve fits provide a gauge frame attached to the graph of an orientation score at each position $g \in SE(2)$ in the 2D-Euclidean motion group and will be used to locally align the diffusion on orientation scores. This locally adaptive alignment of diffusion is a common procedure in image processing, [32], [10], [43], but so far it has always been considered for diffusions directly on images.

The advantage of the more elaborate nonlinear, adaptive diffusions on invertible orientation scores, is that the domain of orientation scores is the $2D$-Euclidean motion group $SE(2)$, which has a much richer structure than the domain of images, $\mathbb{R}^2$, allowing us to deal with (multiple) crossing curves in images.

1.1. *Organization of Part II.* Section 2 gives a quick review of locally adaptive diffusions in image processing. We finish this section with the so-called coherence enhancing diffusions proposed in [43], where both the norm and the direction of the image-gradient is used to steer the diffusion on the image. The basic idea is to diffuse tangent to edges/lines, not orthogonal to edges/lines, in images. The drawback of this approach is that at locations of crossing lines the direction of the gradient is ill-defined resulting in ill-defined orientations and thereby artificial curvatures within the diffusion process. In the orientation score this typical crossing problem is automatically tackled as crossing line structures are torn apart by multiple convolutions with rotated versions of the oriented wavelet. Now in contrast to the differential structure in an image, the direction of each disentangled elongated structure in an orientation score is well-defined. Therefor, in section 4 we consider coherence enhancing diffusion on invertible orientation scores, meaning that we set Φ to be equal to a nonlinear left-invariant diffusion operator with a certain stopping time. Before we can provide these nonlinear diffusions we need some prerequisites from differential geometry on the Euclidean Motion group. This differential geometry will be explained in section 3 and will be used to properly include orientation score adaptive features such as local curvature and deviation from horizontality in our non-linear diffusion schemes.

Section 3 is organized as follows. In subsection 3.1 we reformulate the coherence enhancing diffusion schemes, to stress the role of an invariant metric in an adaptive non-linear diffusion scheme. Then in Section 3.2 we consider the design of an invariant metric on $SE(2)$, where by Theorem 3.1 we must choose between bi-invariance and non-degeneracy. Although bi-invariance is a common requirement in both the fields of mathematics (on symmetric Riemannian spaces, [26]) and computer vision [3], [4], [35], we show why we do *not* need it. As we explain in Lemma 3.3 and Corollary 3.4 operators Φ on orientation scores should be left-invariant and *not* right-invariant.

This brings us to a non-degenerate first fundamental form $\mathcal{G}_\beta$ (inducing a metric) on $SE(2)$, depending on a parameter β with physical dimension $1/[Length]$. The induced metric does not coincide with the usual degenerate bi-invariant Cartan-metric on $SE(2)$. Within this first fundamental form the parameter $\beta > 0$ sets a balance between penalization of length and penalization of curvature of projections of curves to the spatial plane. As β tends to zero this left-invariant inner product tends to the bi-invariant degenerate Cartan metric on $SE(2)$. For $\beta > 0$ this first fundamental form is related to the non-degenerate Cartan metric on $SO(3)$ which can be embedded in $SE(2)$ as we will explain in Theorem 3.2. Furthermore in subsection 3.2 we apply the Maurer-Cartan form and the thereby induced Cartan connection on $SE(2)$. This yields the covariant derivatives of vector fields on $SE(2)$, which we explain in Theorem 3.8. Then in Theorem 3.9 we show that our non-linear diffusions on orientation scores can be expressed in these covariant derivatives and thereby the diffusions take place along the covariantly constant (i.e. auto-parallel) curves, which coincide with the exponential curves on $SE(2)$. The Cartan connection has constant curvature and torsion and so have the auto-parallel curves, which are indeed circular spirals.

Then in subsection 3.3 we consider the definition and relevance of horizontal curves in $SE(2)$. To every C^1-curve $s \mapsto (x(s), y(s))$ one can associate a unique horizontal curve in $SE(2)$ by $s \mapsto (x(s), y(s), \theta(s) = \arg(x'(s) + i\, y'(s)))$. This is relevant, since at regions $\Omega \subset SE(2)$ with strongly oriented responses $|\mathcal{W}_\psi f(g)|$, $g \in \Omega$, in the orientation score $g \mapsto \mathcal{W}_\psi f(g)$ one would like to diffuse mainly along such horizontal curves. We will show that this requires a principal fiber bundle structure P_Y on the domain of an orientation score, constructed from the unique subgroup $Y = \{(0, y, 0) \mid y \in \mathbb{R}\} \subset SE(2)$ with the property that constant right action on a horizontal curves again yields a horizontal curve. On this principal fiber bundle $P_Y = (SE(2), SE(2)/Y, \pi, R)$, with $Y = \{(0, y, 0) \mid y \in \mathbb{R}\}$ and $\pi(g) = gY$ and $R_h g = gh$ we impose a Cartan-Ehresmann connection form. By definition, the kernel of this Cartan-Ehresmann connection form equals the horizontal part of each tangent space $T_g(SE(2))$ and coincides with the tangent space of all horizontal curves through g. This is explained in Theorem 3.13, where we also equip P_Y with the following left-invariant form $\mathrm{d}\theta\otimes\mathrm{d}\theta+\beta^2(\cos\theta\mathrm{d}x+\sin\theta\mathrm{d}y)\otimes(\cos\theta\mathrm{d}x+\sin\theta\mathrm{d}y)$, again parameterized by β, yielding a suitable left-invariant metric on $SE(2)$. This parameter is similar to the natural parameter in elastica curves, [31]. Although there is a difference between the geodesics in P_Y and elastica curves on $SE(2)$, we note that there is a also a strong analogy between these curves, for more details see [17]. Here we will not go into too much detail in the comparison between elastica curves in $\mathbb{R}^2$ and geodesics in P_Y. We just derive the geodesics in P_Y in Appendix A. In contrast to well-known formulas for elastica curves, [31] our exact formula for the geodesics does not involve special functions.

In subsection 3.4 we explain how one can obtain a best (horizontal) exponential curve fit to the orientation score data, locally at each $g \in SE(2)$. Later on in subsection 4.1 we use the tangent vector of these optimal exponential curves to introduce a gauge-coordinate frame of left-invariant vector fields $\{\partial_a, \partial_b, \partial_c\}$ where ∂_b is aligned with the best fitting (horizontal) exponential curve and ∂_a and ∂_c are tangent vectors orthogonal to ∂_b with respect to the first fundamental form $\mathcal{G}_\beta$ of section 3.2.

Finally, in section 4 we use the theoretical results of the previous section in our solution to the well-known medical image analysis problem of enhancement of (multiple) crossing elongated structures in noisy images. For details on the algorithmic side and medical image analysis applications see our applied companion paper [22].

2. Previous work in the field of image analysis on locally adaptive diffusion.

A scale space representation $u_f : \mathbb{R}^d \times \mathbb{R}^+ \to \mathbb{R}$ of an image $f : \mathbb{R}^d \to \mathbb{R}$ is usually obtained by solving an evolution equation on the additive group $(\mathbb{R}^d, +)$. The most common evolution equation, in image analysis, is the diffusion equation,

$$\begin{cases} \partial_s u_f(\mathbf{x}, s) = \nabla_{\mathbf{x}} \cdot (C(u_f(\cdot, s))(\mathbf{x})\, \nabla_{\mathbf{x}} u_f)(\mathbf{x}, s) \\ u_f(\mathbf{x}, 0) = f(\mathbf{x}), \end{cases}$$

where $C : \mathbb{L}_2(\mathbb{R}^2) \cap C^2(\mathbb{R}^2) \to C^1(\mathbb{R}^2)$ is a function which takes care of adaptive conductivity, that is $C(u_f(\cdot, s))(\mathbf{x})$ models the conductivity depending on the local differential structure at $(\mathbf{x}, s, u_f(\mathbf{x}, s))$. If $C = 1$ the solution is given by convolution $u_f(\mathbf{x}, s) = (G_s * f)(\mathbf{x})$ with a Gaussian kernel $G_s(\mathbf{x}) = \frac{1}{(4\pi s)^{\frac{d}{2}}} e^{-\frac{\|\mathbf{x}\|}{4s}}$ with scale, $s = \frac{1}{2}\sigma^2 > 0$.

As pointed out by Perona and Malik [33], nonlinear image adaptive isotropic diffusion is achieved by replacing $C = 1$ by $C(u_f(\cdot, s))(\mathbf{x}) = c(\|\nabla_{\mathbf{x}} u_f(\mathbf{x}, s)\|)$, where $c : \mathbb{R}^+ \to \mathbb{R}^+$ is some smooth strictly decaying positive function vanishing at infinity. This is based on the idea that if (locally) the gradient is large you do not want to diffuse too much. By restricting ourselves to positively valued $c > 0$ one ensures that the diffusion is always forward, and thereby ill-posed backward diffusion is avoided. The common choices are

$$c(t) = e^{-\frac{c}{\left(\frac{\lambda}{t}\right)^{2p}}}, \quad c(t) = \frac{1}{\left(\frac{t}{\lambda}\right)^{2p} + 1} \text{ and } c(t) = \frac{1}{\sqrt{\left(\frac{t}{\lambda}\right)^2 + 1}}, \tag{2.1}$$

involving parameters $p > \frac{1}{2}, \lambda > 0$. The corresponding flux magnitude functions are given by $\phi(t) = t\, c(t),$ with $t = \|\nabla u_f\|$. Now the sign of

$$\phi'(t) = c(t) + tc'(t) \tag{2.2}$$

is important, since if $\phi'(t) > 0$ then the magnitude $\phi(t)$, $t = \|\nabla u_f\|$, of the flux

$$c(\|\nabla u_f\|)\nabla u_f \tag{2.3}$$

(by Gauss Theorem) increases as $\|\nabla u_f\|$ increases, whereas if $\phi'(t) < 0$ the magnitude $\phi(\|\nabla u_f\|)$ of the flux (2.3) decreases as $\|\nabla u_f\|$ increases. Typically, this introduces an extra "sharpening effect" of lines and edges. However, this sharpening effect should not be mistaken for ill-posed backward diffusion because in all cases $c(t) \geq 0$ for all $t > 0$. To this end we note that the Perona and Malik equation can be rewritten in gauge-coordinates $\{a, b\}$, with a along the normalized gradient $\frac{1}{\|\nabla u_f\|}\nabla u_f$ and b along the normalized vector $\frac{1}{\|\nabla u_f\|}(-\partial_y u_f, \partial_x u_f)$ orthogonal to the gradient, using (2.2):

$$\begin{aligned} \frac{\partial u_f}{\partial s} &= \mathrm{div}(c(\|\nabla u_f\|)\nabla u_f) = \frac{\partial}{\partial a}\left(c(\tfrac{\partial u_f}{\partial a})\frac{\partial u_f}{\partial a}\right) + c(\tfrac{\partial u_f}{\partial a})\frac{\partial^2 u_f}{\partial b^2} \quad \Leftrightarrow \\ \frac{\partial u_f}{\partial s} &= \phi'(\tfrac{\partial u_f}{\partial a})\ \frac{\partial^2 u_f}{\partial a^2} + c(\tfrac{\partial u_f}{\partial a})\frac{\partial^2 u_f}{\partial b^2}\ , \end{aligned} \tag{2.4}$$

with $\frac{\partial^2 u_f}{\partial a^2} = \frac{1}{\|\nabla_{\mathbf{x}} u_f\|^2}(\nabla_{\mathbf{x}} u_f) H_{\mathbf{x}}[u_f](\nabla_{\mathbf{x}} u_f)^T$ and $\frac{\partial u_f}{\partial a} = \|\nabla_{\mathbf{x}} u_f\|$.

A further improvement of the Perona and Malik scheme is introduced by Weickert [43], who also uses the *direction* of the gradient $\nabla_{\mathbf{x}} u_f$ of u_f, which is not used in the algorithms of Perona and Malik type. He proposed "coherence enhancing diffusion" (CED) where the diffusion constant c is replaced by a diffusion matrix:

$$\begin{aligned} &S(u_f(\cdot,s))(\mathbf{x}) = (G_\sigma * \nabla u_f(\cdot,s)(\nabla u_f(\cdot,s))^T)(\mathbf{x}), \\ &C(u_f(\cdot,s))(\mathbf{x}) = \alpha I + \\ &(1-\alpha) e^{-\frac{c}{(\lambda_1(S(u_f(\cdot,s))(\mathbf{x})) - \lambda_2(S(u_f(\cdot,s))(\mathbf{x})))^2}}\, \mathbf{e}_2(S(u_f(\cdot,s))(\mathbf{x}))\, \mathbf{e}_2^T(S(u_f(\cdot,s))(\mathbf{x})) \end{aligned} \tag{2.5}$$

where $\alpha \in (0,1)$, $c > 0, \sigma > 0$ are parameters and where the so-called "structure tensor" S, with eigenvalues $\{\lambda_i(S(u_f(\cdot,s))(\mathbf{x}))\}_{i=1,2}$ is used to get a measure for local anisotropy $e^{-\frac{c}{(\lambda_1(S(u_f(\cdot,s))(\mathbf{x})) - \lambda_2(S(u_f(\cdot,s))(\mathbf{x})))^2}}$ together with an orientation estimate $\mathbf{e}_2(S(u_f(\cdot,s))(\mathbf{x}))$, which is the eigenvector of the structure tensor with smallest eigenvalue. In order to get robust orientation estimates it is essential to apply a componentwise smoothing on the so-called "structure-tensor field" $\nabla u_f \otimes \nabla u_f$. The amount of averaging of the structure tensor field is determined by $\sigma > 0$. This leads to useful and visually appealing diffusions of for example the famous Van Gogh paintings and fingerprint images, see Figure 2.

Nevertheless, this method fails in image analysis applications with crossing curves as it starts to create strong artificial curvatures at crossing locations where the direction of the gradient is ill-defined. As this is a major drawback in many imaging applications we are going to solve this problem by considering similar nonlinear adaptive evolution equations on invertible orientation scores. This coherence-enhancing diffusion via invertible orientation scores has two advantages over coherence-enhancing diffusion on images:

(1) In the domain $SE(2) = \mathbb{R}^2 \rtimes \mathbb{T}$ of an (invertible) orientation score $\mathcal{W}_\psi f : SE(2) \to \mathbb{R}$ crossing curves visible in (the sampling of) an image $f : \mathbb{R}^2 \to \mathbb{R}$ are torn apart by convolution with an oriented wavelet at multiple angles (1.2). Along (the spatial projections of) the separated curves the direction of the gradient is well defined. This allows us to diffuse coherently along the separate curves after which the inverse wavelet transformation will automatically merge the separate curves visible in (the sampling of) a diffused orientation score $\Phi(\mathcal{W}_\psi f)$ into a properly smoothed crossing visible in (the sampling of) enhanced image $\Upsilon_\psi(f)$.

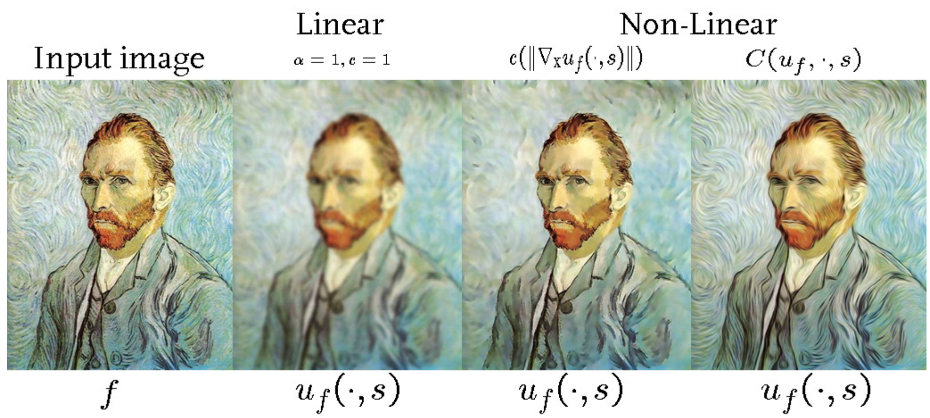

FIG. 2. From left to right: input image f of the well-known portret of Van Gogh, computed on comparable slices $u_f(\cdot, s)$ in a linear scale space representation $C = 1$, Perona en Malik nonlinear scale space representation (left case in (2.1)) and coherence enhancing diffusion (CED) given by (2.5) by Weickert, [43].

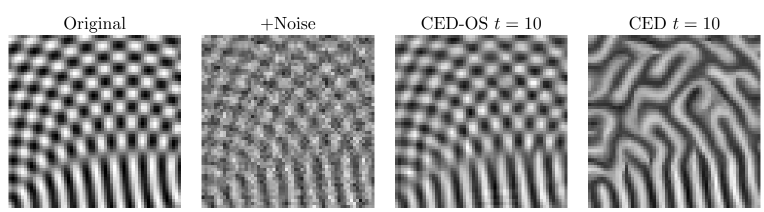

FIG. 3. Illustration of the typical different behavior of coherence enhancing diffusion on images (CED) and coherence enhancing diffusion via invertible orientation scores (CED-OS). Both methods are applied to the second image with noise and both evolutions are stopped at comparable stopping time $t = 10$. Clearly, CED-OS-preserves crossings of curves much better than CED (which creates artistic van Gogh-type of patterns at crossings).

(2) In an orientation score $(x, y, e^{i\theta}) \mapsto \mathcal{W}_\psi(f)(x, y, e^{i\theta})$ we have explicit information on local directions and we can easily measure curvature in a robust manner as we will explain in subsection 3.4. This enables us to align the left-invariant diffusion $\mathcal{W}_\psi f \mapsto \Phi_t(\mathcal{W}_\psi f)$ on the orientation scores adaptively to the local differential structure in an evolving orientation score $\Phi_t(\mathcal{W}_\psi f)$.

See Figure 3. Before we can exploit these advantages, we need to discuss some prerequisites from differential geometry, which will be the subject of the next section.

3. Differential geometry on $SE(2)$.

3.1. *Why do we need an invariant metric in a non-linear diffusion scheme ? .* In order to generalize the CED (coherence enhancing diffusion) schemes to Gabor transforms, analogue to our previous generalization to invertible orientation score, we simply have to replace the left-invariant vector fields $\{\partial_{x_i}\}_{i=1}^d$ on $\mathbb{R}^d$, $d = 2$, by the left-invariant vector fields on $SE(2)$. To this end we formulate the standard coherence enhancing diffusion equations on images (with conductivity (2.5)) as

$$\begin{cases} \partial_s u_f(\mathbf{x},s) & = \left(\nabla_{\mathbf{x}} \cdot \underset{\epsilon\leftarrow\alpha}{S} \begin{pmatrix} \varepsilon & 0 \\ 0 & (1-\varepsilon)e^{-\frac{c}{\lambda_1-\lambda_2}}+\varepsilon \end{pmatrix} \underset{\alpha\leftarrow\epsilon}{S} (\nabla_{\mathbf{x}} u_f(\cdot,s))^T \right)(\mathbf{x}) \\ & = \begin{pmatrix} \partial_a & \partial_b \end{pmatrix} \begin{pmatrix} \varepsilon & 0 \\ 0 & (1-\varepsilon)e^{-\frac{c}{(\lambda_1-\lambda_2)^2}}+\varepsilon \end{pmatrix} \begin{pmatrix} \partial_a \\ \partial_b \end{pmatrix} u_f(\mathbf{x},s), \quad \mathbf{x}\in\mathbb{R}^2, s>0, \\ u_f(\mathbf{x},0) & = f(\mathbf{x}), \qquad \mathbf{x}\in\mathbb{R}^2. \end{cases} \tag{3.1}$$

with the global standard basis $\epsilon = \{\mathbf{e}_x, \mathbf{e}_y\} := \{(1,0),(0,1)\} \leftrightarrow \{\partial_x, \partial_y\}$ and the (locally adapted) basis of eigen vectors of help-matrix $S(u_f(\cdot,s))(\mathbf{x})$:

$$\alpha = \{\mathbf{e}_1, \mathbf{e}_2\} := \{\mathbf{e}_1\left(S(u_f(\cdot,s))(\mathbf{x})\right), \mathbf{e}_2\left(S(u_f(\cdot,s))(\mathbf{x})\right)\} \leftrightarrow \{\partial_a, \partial_b\},$$

with respective eigen values $\lambda_k := \lambda_k(S(u_f(\cdot,s))(\mathbf{x}))$, $k=1,2$ of the so-called structure tensor $S(u_f(\cdot,s))(\mathbf{x})$ at position $\mathbf{x}\in\mathbb{R}^2$ at time $s>0$. The corresponding orthogonal basis transform $\left(\underset{\alpha\leftarrow\epsilon}{S}\right)^T = \underset{\epsilon\leftarrow\alpha}{S} = (\mathbf{e}_1 \mid \mathbf{e}_2)$ and with $(\partial_a \;\; \partial_b) = (\partial_x \;\; \partial_y)\underset{\epsilon\leftarrow\alpha}{S}$. At isotropic areas $\lambda_1 \to \lambda_2$ and thereby the conductivity matrix becomes a multiple of the identity yielding isotropic diffusion only at isotropic areas which is desirable for noise-removal.

Intuitively, the diffusion matrix is diagonalized with respect to a local Gauge-coordinate frame attached to the graph $\Gamma_{u_f(\cdot,\cdot,s)} = \{(x,y,u_f(x,y,s)) \mid (x,y)\in\mathbb{R}^2\}$ of a (compactly supported) blurred image $(x,y)\mapsto u_f(x,y,s)$, $s\geq 0$. In principle, if f is sufficiently smooth one may consider linear diffusion equations by making the conductivity only adaptive to $f = u_f(\cdot,\cdot,0)$. In such case the mapping $f\mapsto u_f$ is still highly non-linear, but the diffusion equation itself is linear. In a numerical finite difference scheme this means that the conductivity need not be updated as it is not depending on time. Moreover, in this case the diffusion system will have a unique smooth solution. This uniqueness, however, is to our knowledge not a priori guaranteed in the case of non-linear diffusions.

In stead of adapting the conductivity one can also replace the standard first fundamental form on the image domain by a first fundamental form on the graph of an image in order to consider Laplace-Beltrami flow, as proposed by Sochen [35]:

$$\begin{cases} \partial_s u_f(x,y,s) = \frac{1}{\sqrt{\det\{G(x,y,s)\}}} \sum\limits_{i=1}^{3}\sum\limits_{j=1}^{3} \partial_i \left\{ \sqrt{\det\{G(x,y,s)\}}\, G^{ij}(x,y,s)\, \partial_j u_f(\cdot,\cdot,s) \right\}(x,y), \\ \text{where we applied short notation } G(x,y,s) := C(u_f(\cdot,\cdot,s))(x,y), \\ u_f(x,y,s=0) = f(x,y) \text{ for all } (x,y)\in\mathbb{R}^2. \end{cases}$$

Now note that the righthand side in the PDE in (3.1), which can be rewritten as

$$\sum_{i=1}^{3}\sum_{j=1}^{3} \partial_i \left\{ G^{ij}(\cdot,\cdot,s)\partial_j u_f(\cdot,\cdot,s) \right\}(x,y),$$

where $[G^{ij}(x,y,s)]_{i,j=1}^3$ denotes the *inverse* of the first fundamental form matrix $G(x,y,s) = [G_{ij}(x,y,s)]_{i,j=1}^3$ which equals the symmetric positive definite conductivity matrix $C(u_f(\cdot,\cdot,s))(x,y)$, recall (2.5), evaluated at position $(x,y)\in\mathbb{R}^2$ at time $s>0$.

By the product rule for differentiation the Laplace Beltrami-flow can be obtained by adding the following terms to the righthand side of the PDE in (3.1):

$$+\frac{1}{\sqrt{\det G(x,y,s)}} \sum_{i=1}^{3} \partial_i \left\{ \sqrt{\det G(\cdot,\cdot,s)} \right\}(x,y) \sum_{j=1}^{3} G^{ij}(x,y,s)\, \partial_j u_f(x,y,s)\ .$$

For numerical reasons, however, we will *not* add these terms within this paper.

Now in order to generalize the coherence enhancing diffusion schemes on images to coherence enhancing diffusion schemes on orientation scores we must replace the left-invariant vector fields on $\mathbb{R}^2$ by the left-invariant vector fields on $SE(2)$, like in (1.9), and we need an invariant first fundamental form $\mathcal{G}$ on $SE(2)$, rather than the trivial, bi-invariant, first fundamental on $(\mathbb{R}^2, T(\mathbb{R}^2))$, where each tangent space $T_{\mathbf{x}}(\mathbb{R}^2)$ is identified with $T_{\mathbf{0}}(\mathbb{R}^2)$ by standard parallel transport on $\mathbb{R}^2$, i.e. $\mathcal{G}_{\mathbb{R}^2}(\mathbf{x},\mathbf{y}) = \mathbf{x}\cdot\mathbf{y} = x^1y^1 + x^2y^2$.

3.2. *Design of the metric on $SE(2)$: Bi-invariance versus non-degeneracy* . In both the field of image analysis [3] and in mathematics (symmetric spaces) [26] it is very common to use bi-invariant metrics on groups. Here arises the first complication, as in $SE(2)$ no such bi-invariant, non-degenerate, first fundamental form (inducing a metric) exists, see Theorem 3.1. So for the underlying metric in our non-linear diffusion schemes we must choose between bi-invariance and non-degeneracy. In this section we explain why we use a left-invariant, non-degenerate metric on $SE(2)$ as underlying metric for our non-linear diffusions on orientation scores. Furthermore, we will consider somewhat tough differential geometry on $SE(2)$, which serves as an essential prerequisite for full understanding and design of our diffusions on orientation scores later on.[1]

THEOREM 3.1. The only real-valued *left-invariant* (symmetric, positive, semidefinite) first fundamental forms $\mathcal{G} : SE(2) \times T(SE(2)) \times T(SE(2)) \to \mathbb{C}$ on $SE(2)$ are given by

$$\mathcal{G} = \sum_{i=1}^{3}\sum_{j=1}^{3} g_{ij}\ \mathrm{d}\mathcal{A}^i \otimes \mathrm{d}\mathcal{A}^j\ , \qquad g_{ij} \in \mathbb{R}, \tag{3.2}$$

where the dual basis $\{\mathrm{d}\mathcal{A}^1, \mathrm{d}\mathcal{A}^2, \mathrm{d}\mathcal{A}^3\} \subset (\mathcal{L}(SE(2)))^*$ of the dual space $(\mathcal{L}(SE(2)))^*$ of the vector space $\mathcal{L}(SE(2)$ of left-invariant vector fields spanned by

$$\mathcal{A}_1 = \partial_\theta,\ \mathcal{A}_2 = \partial_\xi = \cos\theta\,\partial_x + \sin\theta\,\partial_y,\ \mathcal{A}_3 = \partial_\eta = -\sin\theta\,\partial_x + \cos\theta\,\partial_y, \tag{3.3}$$

obtained by applying the derivative $\mathrm{d}\mathcal{R}$ of the right-regular representation $\mathcal{R}$ to the standard basis in the Lie-algebra $\{A_1, A_2, A_3\} := \{\partial_x, \partial_y, \partial_\theta\} \subset T_e(SE(2))$, is given by

$$\mathrm{d}\mathcal{A}^1 = \mathrm{d}\theta\ ,\quad \mathrm{d}\mathcal{A}^2 = \cos\theta\,\mathrm{d}x + \sin\theta\,\mathrm{d}y,\quad \mathrm{d}\mathcal{A}^3 = -\sin\theta\,\mathrm{d}x + \cos\theta\,\mathrm{d}y. \tag{3.4}$$

The only (up to scalar multiplication) *bi-invariant* fundamental form on $SE(2)$ is degenerate and given by $\mathcal{G} \equiv \mathrm{d}\theta \otimes \mathrm{d}\theta$.

Proof. Recall from part I [18, ch:3] that $\mathrm{d}\mathcal{R}$ yields the fundamental isomorphism between the Lie-algebras $T_e(SE(2))$ and $\mathcal{L}(SE(2))$, so $\mathcal{A}_i = \mathrm{d}\mathcal{R}(A_i)$ and $[A_i, A_j] = [\mathcal{A}_i, \mathcal{A}_j] = \mathcal{A}_i\mathcal{A}_j - \mathcal{A}_j\mathcal{A}_i$. The dual basis (3.4) satisfies $\langle \mathrm{d}\mathcal{A}^i, \mathcal{A}_j\rangle = \delta^i_j$. Then by definition $\mathcal{G}$ is

- left-invariant if $\forall_{h,g\in SE(2)}\forall_{X,Y\in\chi(SE(2))}\ :\ \mathcal{G}_h(X_h, Y_h) = \mathcal{G}_{gh}((L_g)_*X_h, (L_g)_*Y_h)$.
- right-invariant if $\forall_{h,g\in SE(2)}\forall_{X,Y\in\chi(SE(2))}\ :\ \mathcal{G}_h(X_h, Y_h) = \mathcal{G}_{hg}((R_g)_*X_h, (R_g)_*Y_h)$.
- inversion-invariant if $\forall_{h,g\in SE(2)}\forall_{X,Y\in\chi(SE(2))}\ :\ \mathcal{G}_{r_e(g)}((r_e)_*X_g, (r_e)_*Y_g) = \mathcal{G}_g(X_g, Y_g)$.
- Ad-invariant if $\forall_{h,g\in SE(2)}\forall_{X,Y\in\chi(SE(2))}\ :\ \mathcal{G}_{hgh^{-1}}(\mathrm{Ad}(h)\,X_g, \mathrm{Ad}(h)\,X_g) = \mathcal{G}_g(X_g, Y_g)$

[1] It is not crucial to grasp all details in subsections 3.2, 3.3 to follow sections 3.4 and 4. The reader who is not interested in the details can skip all proofs in subsections 3.2, 3.3 and just consider Theorems 3.1, 3.3, 3.4, 3.9 and Definition 3.11 and eq.'s (3.5), (3.11), (3.25), (3.26),(3.31), (3.23), (3.24),(3.38).

- reflection-invariant if $\forall_{h,g\in SE(2)}\forall_{X,Y\in \chi(SE(2))}\ :\ \mathcal{G}_{r_h(g)}((r_h)_* X_g,(r_h)_* Y_g)=\mathcal{G}_g(X_g,Y_g)$.

Now $(T_g(SE(2)))^*$ is spanned by $\{\,\mathrm{d}\mathcal{A}^1\big|_g, \mathrm{d}\mathcal{A}^2\big|_g, \mathrm{d}\mathcal{A}^3\big|_g\}$ for all $g\in SE(2)$. As a result for all $g\in SE(2)$ there exist numbers $g_{ij}(g)\in\mathbb{R}$, $i,j=1,2,3$ such that

$$\mathcal{G}_g=\sum_{i=1}^{3}\sum_{j=1}^{3} g_{ij}(g)\ \ \mathrm{d}\mathcal{A}^i\Big|_g\otimes \mathrm{d}\mathcal{A}^j\Big|_g .$$

Now $\mathcal{G}$ is left-invariant iff $\forall_{i,j\in\{1,2,3\}}\forall_{g\in SE(2)}\ \mathcal{G}_g(\mathcal{A}_i|_g, \mathcal{A}_j|_g)=\mathcal{G}_e((L_{g^{-1}})^*\ \mathcal{A}_i|_g, (L_{g^{-1}})^*\ \mathcal{A}_j|_g)=\mathcal{G}_e(A_i,A_j)$, i.e. $\forall_{i,j\in\{1,2,3\}}\forall_{g\in SE(2)}\ g_{ij}(g)=g_{ij}(e)$. Now for the cases where $\mathcal{G}$ is bi-invariant we note that reflections around the unity element given by $r_e(g)=g^{-1}$ relate left multiplication $L_g h=gh$ to right multiplication $R_g h=hg$ since $R_g=r_e L_{g^{-1}} r_e \Leftrightarrow r_e R_{g^{-1}} r_e=L_g$ and reflections $h\mapsto r_g(h)=gh^{-1}g$ around element $g\in SE(2)$ follow by $r_g=L_g R_g r_e$ and the adjoint action is defined by $\mathrm{Ad}(g)=(R_{g^{-1}}L_g)_*$, so that, [37] Ch:V;

$$\begin{aligned}&\mathcal{G}\text{ is both left and inversion-invariant }\Leftrightarrow \mathcal{G}\text{ is both left and right-invariant}\\ &\Leftrightarrow \mathcal{G}\text{ is both left and reflection-invariant }\Leftrightarrow \mathcal{G}\text{ is both left and Ad-invariant}\ .\end{aligned}$$

This brings us[2] to the left-invariant Cartan form induced by the Killing-form K (which is invariant under all Lie algebra automorphisms, [26] p.266 in particular Ad):

$$\begin{aligned}\mathcal{G}_g &= -K(A_i,A_j)\ \ \mathrm{d}\mathcal{A}^i\big|_g\otimes \mathrm{d}\mathcal{A}^j\big|_g=\mathrm{trace}\left(\mathrm{ad}(\mathcal{A}_i)\circ \mathrm{ad}(\mathcal{A}_j)\right)\ \ \mathrm{d}\mathcal{A}^i\big|_g\otimes \mathrm{d}\mathcal{A}^j\big|_g\\ &= -\langle \mathrm{d}\mathcal{A}^k, \mathrm{ad}(\mathcal{A}_i)\circ \mathrm{ad}(\mathcal{A}_j)A_k\rangle\ \ \mathrm{d}\mathcal{A}^i\big|_g\otimes \mathrm{d}\mathcal{A}^j\big|_g=-c^l_{kj}c^k_{li}\ \mathrm{d}\mathcal{A}^i\big|_g\otimes \mathrm{d}\mathcal{A}^j\big|_g\ ,\end{aligned} \tag{3.5}$$

where c^k_{ij} are the structure constants of the Lie-algebra and $\mathrm{ad}(\mathcal{A}_j)\mathcal{A}_i=[\mathcal{A}_i,\mathcal{A}_j]=c^k_{ij}\mathcal{A}_k$. Direct computation of this Killing form yields $\mathcal{G}=\mathrm{d}\theta\otimes\mathrm{d}\theta$. It is not difficult to see that the metric given in (3.5) is the only both left- and Ad-invariant metric, since by left-invariance it can be written as (3.2) and by $\mathrm{Ad}_{g=(x,y,e^{i\theta})}(\partial_\theta)=\partial_\theta - y\ \partial_x + x\ \partial_y$, $\mathrm{Ad}_{(x,y,e^{i\theta})}(\partial_x)=\partial_x$, $\mathrm{Ad}_{(x,y,e^{i\theta})}(\partial_y)=\partial_y$, the adjoint orbits are planes with fixed ∂_θ component on which the quadratic form is constant, so $g_{ij}=0$ if $i\neq 1$ and $j\neq 1$. □

So we must choose between bi-invariance and invertibility. On the one hand, in Lie group theory it is common to maintain bi-invariance and therefor we embed $SE(2)$ into $SO(3)$, on which the bi-invariant metric is non-degenerate. In Theorem 3.2 we present a parameterized class of compact groups $\{(SE(2))^\beta \mid 0<\beta\leq 1\}$, with $\lim\limits_{\beta\downarrow 0}(SE(2))^\beta = SE(2)$ and $(2\pi\mathbb{Z}\times\{0\}\times\{0\})\backslash(SE(2))^{\beta=1}\equiv SO(3)$. Each member of this class admits a bi-invariant metric which is non-degenerate iff $\beta>0$. We use this class to derive covariant derivatives and Riemannian curvature on $(SE(2))^\beta$ and by taking the limit $\beta\downarrow 0$ we obtain covariant derivatives and sectional curvatures on $SE(2)$. On the other hand operators on orientation scores should be left-invariant, *not* right-invariant, so we do not need right-invariance. This follows by Lemma 3.3 and Corollary 3.4.

THEOREM 3.2. The Euclidean motion group $SE(2)$ can be obtained by contraction from the group $SO(3)$, by means of the groups[3] $(SE(2))^\beta$, $\beta\in[0,1]$, that arise by equipping

[2]Occasionally within this paper, like in (3.5), we use the Einstein summation convention, i.e. we apply automatic summation over indices which appear both as upper and lower index.

[3]The groups $(SE(2))^\beta$, $\beta\in[0,1]$ in this part II, connecting $SE(2)$ and $SO(3)$, should not be mistaken with the groups $(SE(2))_t$, $t\in[0,1]$, connecting $SE(2)$ and $H(3)$, used in part I [18].

the set $\mathbb{R}^2 \times S_1$ with group product

$$\begin{aligned}(x,y,\theta)\cdot_\beta (x',y',\theta') &= (x + x'\cos\theta\sqrt{1+\beta^2y^2} - y'\sin\theta\sqrt{1+\beta^2y^2}\ ,\ y + x'(1+\beta^2y^2)\sin\theta + y'(1+\beta^2y^2)\cos\theta, \\ &\quad \theta+\theta' - \beta^2 x' y\cos\theta + \beta^2 y' y \sin\theta \quad \text{Mod } 2\pi)\ .\end{aligned}$$

One has $SE(2) = \lim\limits_{\beta\downarrow 0}(SE(2))^\beta$ and[4] $SO(3) \equiv 2\pi\mathbb{Z}\times\{0\}\times\{0\}\backslash (SE(2))^{\beta=1}$. The latter isomorphism (for geometrical explanation see Figure 4) is given by

$$\begin{array}{l} SO(3) \ni R_{\mathbf{e}_z,\tilde{\gamma}}R_{\mathbf{e}_y,\tilde{\beta}}R_{\mathbf{e}_z,\tilde{\alpha}} \ \leftrightarrow\ (x,y,\theta)\in (SE(2))^{\beta=1} \\ \Leftrightarrow \tilde{\alpha} = x \text{ and } \tilde{\beta} = \frac{\pi}{2} - \arctan(y) \text{ and } \tilde{\gamma} = \theta. \end{array} \tag{3.6}$$

where the well-known Euler angle parametrization of $SO(3)$ is given by $R_{\mathbf{e}_z,\tilde{\gamma}}R_{\mathbf{e}_y,\tilde{\beta}}R_{\mathbf{e}_z,\tilde{\alpha}}$. The left-invariant vector fields on $(SE(2))^\beta$ are given by

$$\begin{aligned} \mathcal{A}_1^\beta &= \partial_\theta\ , \\ \mathcal{A}_2^\beta &= -\beta^2 y\cos\theta\,\partial_\theta + \cos\theta\,\sqrt{1+\beta^2\,y^2}\,\partial_x + \sin\theta\,(1+\beta^2\,y^2)\,\partial_y\ , \\ \mathcal{A}_3^\beta &= \beta^2 y\sin\theta\,\partial_\theta - \sin\theta\,\sqrt{1+\beta^2\,y^2}\,\partial_x + \cos\theta\,(1+\beta^2\,y^2)\,\partial_y\ . \end{aligned} \tag{3.7}$$

These vector fields form a 3D-Lie algebra : $[\mathcal{A}_1^\beta,\mathcal{A}_2^\beta] = \mathcal{A}_3^\beta,\ [\mathcal{A}_1^\beta,\mathcal{A}_3^\beta] = -\mathcal{A}_2^\beta,\ [\mathcal{A}_2^\beta,\mathcal{A}_3^\beta] = \beta^2\,\mathcal{A}_1^\beta$. which tends to $\mathcal{L}(SE(2)) = \{\partial_\theta,\partial_\xi,\partial_\eta\}$ for $\beta\to 0$. Let the left-invariant co-vectors $\{\mathrm{d}\mathcal{A}^i_\beta\}_{i=1}^3$ be given by $\langle \mathrm{d}\mathcal{A}^i_\beta, \mathcal{A}^\beta_j\rangle = \delta^i_j$, then the bi-invariant metric $\mathcal{G}^\beta$ on $(SE(3))^\beta$ induced by the Killing form (like in (3.5)) is given by

$$\mathcal{G}^\beta = g_{ij}\mathrm{d}\mathcal{A}^i_\beta\otimes \mathrm{d}\mathcal{A}^j_\beta, \text{ with } G = [g_{ij}] = \begin{pmatrix} 1 & 0 & 0 \\ 0 & \beta^2 & 0 \\ 0 & 0 & \beta^2 \end{pmatrix}. \tag{3.8}$$

As a result the groups $(SE(2))^\beta$ are compact symmetric[5] Riemannian spaces iff $\beta > 0$. The Riemann curvature tensor on these symmetric Riemannian spaces equals:

$$\begin{aligned} R &= \beta^2\mathcal{A}_1^\beta\otimes \mathrm{d}\mathcal{A}^2_\beta\otimes \mathrm{d}\mathcal{A}^1_\beta\wedge \mathrm{d}\mathcal{A}^2_\beta - \beta^2\mathcal{A}_1^\beta\otimes \mathrm{d}\mathcal{A}^3_\beta\otimes \mathrm{d}\mathcal{A}^1_\beta\wedge \mathrm{d}\mathcal{A}^3_\beta \\ &\quad + \beta^2\mathcal{A}_2^\beta\otimes \mathrm{d}\mathcal{A}^3_\beta\otimes \mathrm{d}\mathcal{A}^2_\beta\wedge \mathrm{d}\mathcal{A}^3_\beta - \beta^2\mathcal{A}_3^\beta\otimes \mathrm{d}\mathcal{A}^2_\beta\otimes \mathrm{d}\mathcal{A}^3_\beta\wedge \mathrm{d}\mathcal{A}^2_\beta \\ &\quad + \mathcal{A}_2^\beta\otimes \mathrm{d}\mathcal{A}^1_\beta\otimes \mathrm{d}\mathcal{A}^1_\beta\wedge \mathrm{d}\mathcal{A}^2_\beta \ + \ \mathcal{A}_3^\beta\otimes \mathrm{d}\mathcal{A}^1_\beta\otimes \mathrm{d}\mathcal{A}^1_\beta\wedge \mathrm{d}\mathcal{A}^3_\beta\ . \end{aligned} \tag{3.9}$$

Proof. The tangent space space at unity element $e = (0,0,0)$ of all groups $\{(SE(2))_\beta\}$ is the same for all $\beta\geq 0$ and it is spanned by $\{A_1,A_2,A_3\} = \{\partial_x,\partial_y,\partial_\theta\}$. Now the formula for the left-invariant invariant vector field $\mathcal{A}_i^\beta$ (3.7) directly follows by applying the derivative $\mathrm{d}\mathcal{R}$ of the right-regular representation $\mathcal{R}$ given by $\mathcal{R}_g\phi(h) = \phi(hg)$, like in (B.2), to A_i, $i=1,2,3$. Now with respect to isomorphism (3.6) we note that the Euler angle parametrization of $SO(3)$ is given by $R_{\mathbf{e}_z,\tilde{\gamma}}R_{\mathbf{e}_y,\tilde{\beta}}R_{\mathbf{e}_z,\tilde{\alpha}}$. A basis of left-invariant vector fields on $SO(3)$ (in Euler-angles) is given by

$$\mathcal{B}_1 = \cot\tilde{\beta}\cos\tilde{\gamma}\,\partial_{\tilde{\gamma}} - \tfrac{\cos\tilde{\gamma}}{\sin\tilde{\beta}}\,\partial_{\tilde{\alpha}} + \sin\tilde{\gamma}\,\partial_{\tilde{\beta}}, \quad \mathcal{B}_2 = -\cot\tilde{\beta}\,\sin\tilde{\gamma}\,\partial_{\tilde{\gamma}} - \tfrac{\cos\tilde{\gamma}}{\sin\tilde{\beta}}\,\partial_{\tilde{\alpha}} + \sin\tilde{\gamma}\,\partial_{\tilde{\beta}}, \tag{3.10}$$

and $\mathcal{B}_3 = \partial_{\tilde{\gamma}}$, with commutators $[\mathcal{B}_1,\mathcal{B}_2] = \mathcal{B}_3, [\mathcal{B}_2,\mathcal{B}_3] = \mathcal{B}_1$, $[\mathcal{B}_3,\mathcal{B}_1] = \mathcal{B}_2$, [8, ch:9.10]. If we apply the coordinate transformation $\tilde{\alpha} = \beta x$, $\tilde{\beta} = \frac{\pi}{2} - \arctan(\beta y)$, $\tilde{\gamma} = \theta$ and multiply $\mathcal{B}_1$ and $\mathcal{B}_2$ with β we obtain the left-invariant vector fields (3.7). Therefore these vector fields $\{\mathcal{A}_1^\beta,\mathcal{A}_2^\beta,\mathcal{A}_3^\beta\}$ again form a three dimensional Lie algebra:

$$[\mathcal{A}_1^\beta,\mathcal{A}_2^\beta] = \mathcal{A}_3^\beta, \quad [\mathcal{A}_1^\beta,\mathcal{A}_3^\beta] = -\mathcal{A}_2^\beta, \quad [\mathcal{A}_2^\beta,\mathcal{A}_3^\beta] = \beta^2\,\mathcal{A}_1^\beta.$$

[4] The quotient is taken only to ensure the first variable x of the group $(SE(2))^{\beta=1}$ is 2π-periodic.
[5] These spaces are symmetric with respect to fundamental reflection $h\mapsto gh^{-1}g$, [26].

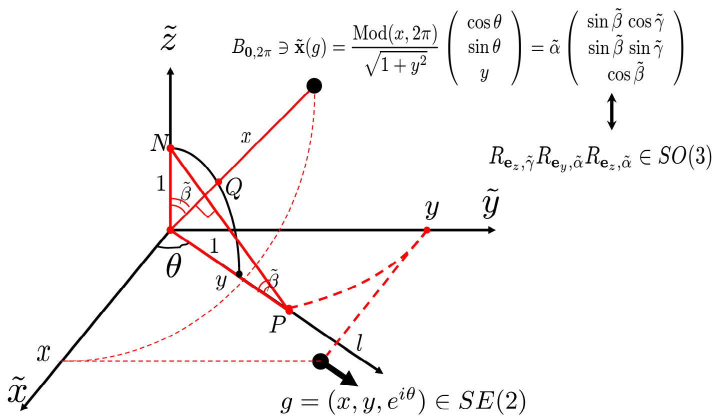

FIG. 4. The embedding of $SE(2)$ in $SO(3)$ by (3.6) for $\beta = 1$. The group $SO(3)$ can be identified with a unit ball $B_{\mathbf{0},2\pi}$ with radius 2π by means of the Euler angle parametrization. Here all points on the sphere $\{\tilde{\mathbf{x}} \in \mathbb{R}^3 \mid \|\tilde{\mathbf{x}}\| = \tilde{\alpha} = 2\pi\}$ are identified with the origin. Now given a fixed member of $(x, y, e^{i\theta}) \in SE(2)$ we can obtain the corresponding element in $SO(3)$ as follows. First consider the point $(\tilde{x}, \tilde{y}, \tilde{z}) = (x, y, 0)$ with attached direction $\theta = \angle((\tilde{x}, \tilde{y}), (1, 0))$ and construct the unique half-line ℓ trough the origin with direction θ. Then project $(x, y, 0)$ on the $\tilde{y}$-axis and rotate the point so that it ends up at point P at the line ℓ. Then find the unique point Q on the unit sphere such that $\vec{OQ} \perp \vec{PN}$ where N is the north-pole. Finally, scale Q with x modulo 2π.

which converges to $\{\mathcal{A}_1, \mathcal{A}_2, \mathcal{A}_3\} = \{\partial_\theta, \partial_\xi, \partial_\eta\}$ for $\beta \to 0$. Now the Lie-algebra of $SO(3)$ is equal to $so(3) = \{A \in GL(3, \mathbb{R}) \mid A^T = -A\}$ which is isomorphic to $\mathbb{R}^3$ by means of $\mathbf{a} \leftrightarrow \mathbf{x} (\mapsto \mathbf{a} \times \mathbf{x})$ and by direct computation of (3.5) we indeed find $g_{ij}^{\beta=1} = \delta_{ij}$ and (3.8). Moreover (3.9) follows by Cartan's formula [1] for the Riemannian curvature tensor-components on compact, semi-simple Lie-groups: $R^i_{j,kl} = \frac{1}{2}\sum_\lambda c^i_{\lambda j} c^\lambda_{kl}$, where $-c^2_{13} = c^2_{31} = c^3_{12} = -c^3_{21} = 1$ and $c^1_{23} = \beta^2$. As a matrix group is compact and semi-simple iff its Killing form is negative-definite, [26, p.269], $(SE(2))_\beta$ is compact iff $\beta > 0$. However, Cartan's formula also applies to the case $\beta = 0$ as we show in Appendix B. □

LEMMA 3.3. Let Φ be a mapping on the space of orientation scores $\Phi : \mathbb{C}_K^{SE(2)} \to \mathbb{C}_K^{SE(2)}$. Let $\Upsilon_\psi = \mathcal{W}_\psi^* \circ \Phi \circ \mathcal{W}_\psi$ be the corresponding operator on the space $\mathbb{L}_2(\mathbb{R}^2)$ of images. Let $\mathcal{U}$ respectively $\mathcal{L}$ denote the regular representation of $SE(2)$ onto $\mathbb{L}_2(\mathbb{R}^2)$ and $\mathbb{L}_2(SE(2)$, given by respectively (1.1) and $\mathcal{L}_g U(h) = U(g^{-1}h)$.

$$\begin{array}{lcl} \forall_{g \in SE(2)} \;:\; \Phi \circ \mathcal{L}_g = \mathcal{L}_g \circ \Phi & \Leftrightarrow & \forall_{g \in SE(2)} \;:\; \mathcal{U}_g \circ \Upsilon_\psi = \Upsilon_\psi \circ \mathcal{U}_g \;, \\ \forall_{g \in SE(2)} \;:\; \Phi \circ \mathcal{R}_g = \mathcal{R}_g \circ \Phi & \Leftrightarrow & \forall_{g \in SE(2)} \;:\; \Upsilon_{\mathcal{U}_g \psi} = \Upsilon_\psi \;. \end{array} \tag{3.11}$$

Proof. Recall from Figure 1 that every operator Φ on (and in) the space of orientation scores (associated to kernel ψ) is 1-to-1 related to an operator $\Upsilon_\psi = \mathcal{W}_\psi^* \circ \Phi \circ \mathcal{W}_\psi$ on the space of images. Now it is easily verified by conjugation that the following relations hold

$$\begin{array}{lcl} \forall_{g \in SE(2)} \;:\; \mathcal{W}_\psi \mathcal{U}_g = \mathcal{L}_g \mathcal{W}_\psi & \Leftrightarrow & \forall_{g \in SE(2)} \;:\; \mathcal{W}_\psi^* \mathcal{L}_g = \mathcal{U}_g \mathcal{W}_\psi^* \;, \\ \forall_{g \in SE(2)} \;:\; \mathcal{R}_g \mathcal{W}_\psi = \mathcal{W}_{\mathcal{U}_g \psi} & \Leftrightarrow & \forall_{g \in SE(2)} \;:\; \mathcal{W}_\psi^* = (\mathcal{W}_{\mathcal{U}_g \psi})^* \mathcal{R}_g \;, \end{array} \tag{3.12}$$

where we used $(\mathcal{L}_g)^* = (\mathcal{L}_g)^{-1} = \mathcal{L}_{g^{-1}}$, $(\mathcal{R}_g)^* = (\mathcal{R}_g)^{-1} = \mathcal{R}_{g^{-1}}$, $(\mathcal{U}_g)^* = (\mathcal{U}_g)^{-1} = \mathcal{U}_{g^{-1}}$ for all $g \in SE(2)$. Now the result (3.11) directly follows from (3.12). □

COROLLARY 3.4. Operators on orientation scores Φ should be left-invariant (i.e. $\mathcal{L}_g \circ \Phi = \Phi \circ \mathcal{L}_g$) and *not* right-invariant in order to ensure that the net operator Υ_ψ is a Euclidean invariant operator which requires an appropriately centered and rotated anisotropic kernel ψ.

Therefore we consider the Maurer-Cartan form on $SE(2)$, see Theorem 3.8, and impose the following left-invariant, first fundamental form $\mathcal{G}_\beta : SE(2) \times T(SE(2)) \times T(SE(2)) \to \mathbb{C}$ on $SE(2)$,

$$\boxed{\mathcal{G}_\beta = \sum_{i,j=1}^{3} g_{ij} \mathrm{d}\mathcal{A}^i \otimes \mathrm{d}\mathcal{A}^j = \mathrm{d}\theta \otimes \mathrm{d}\theta + \beta^2 \mathrm{d}\mathcal{A}^2 \otimes \mathrm{d}\mathcal{A}^2 + \beta^2 \mathrm{d}\mathcal{A}^3 \otimes \mathrm{d}\mathcal{A}^3 \ ,} \tag{3.13}$$

where $[g_{ij}] = \mathrm{diag}\{1, \beta^2, \beta^2\}$. Here the parameter β (physical dimension equals $1/[Length]$) should be considered as a fundamental parameter which relates distance on the torii $\{(\mathbf{x}, e^{i\theta}) \mid \theta \in [0, 2\pi)\}$ to distances in the spatial planes $\{(\mathbf{x}, e^{i\theta}) \mid \mathbf{x} \in \mathbb{R}^2\}$. We return to this explanation of β later when we put an explicit relation to certain geodesics in $SE(2)$ and elastica curves in $\mathbb{R}^2$ (where β^2 determines the typical energy-ratio of bending and stretching of an elastic rod).

Ironically, this left-invariant metric $\mathcal{G}_\beta$ on $SE(2)$, which serves as the major ingredient in our diffusion schemes on orientation scores in section 4, is clearly related to the bi-invariant metric $\mathcal{G}^\beta$ on the compact group $(SE(2))^\beta$, (3.8).

In order to be able to understand the full meaning of the next two theorems we need some basic definitions from differential geometry.

DEFINITION 3.5. Let M be a smooth manifold, G be a Lie-group. A principal fiber bundle $P_G := (P, M, \pi, R)$ above a manifold M with structure group G is a tuple (P, M, π, R) such that. P is a smooth manifold, $\pi : P \to M$ is a smooth projection map with $\pi(P) = M$, R a smooth right action $R_g p = p \cdot g$, $p \in P$, $g \in G$, such that $p \cdot (gh) = (p \cdot g) \cdot h$ and $\pi(p \cdot g) = \pi(p)$ for all $p \in P$, $g, h \in G$. Finally it should satisfy the "local triviality" condition, [36, p.346-347].

DEFINITION 3.6. It is common to equip a principal fiber bundle $P_G = (P, M, \pi, R)$ with an Cartan-Ehresmann connection form ω. This is by definition a Lie-algebra $T_e(G)$-valued 1-form $\omega : P \times T(P) \to T_e(G)$ on P such that

$$\begin{aligned} &\omega(\mathrm{d}\mathcal{R}(A)) = A \text{ for all } A \in T_e(G), \\ &\omega((R_h)_* \mathcal{A}) = \mathrm{Ad}(h^{-1})\omega(\mathcal{A}) \text{ for all vector fields } \mathcal{A} \text{ and all } g \in G \ . \end{aligned} \tag{3.14}$$

It is also common practice to relate principal fiber bundles to vector bundles. Here one uses an external representation $\rho : G \to F$ into a finite dimensional vector space F of the structure group to put an appropriate vector space structure on the fibers $\{\pi^{-1}(m) \mid m \in M\}$ in the principal fiber bundles.

DEFINITION 3.7. Let P be a principal fiber bundle with finite dimensional structure group G. Let $\rho : G \to F$ be a representations in a finite dimensional vector space F. Then the associated vector bundle is denoted by $P \times_\rho F$ and equals the orbit space under the right action

$$(P \times F) \times G \to P \times F \text{ given by } ((u, X), g) \mapsto (ug, \rho(g)X),$$

for all $g \in G$, $X \in F$ and $u \in P$.

For details on the associated fiber bundle see [34, p.123–148], where at the end the author provides a clarifying table of correspondences between P and $P \times_\rho F$.

THEOREM 3.8. The Maurer-Cartan form ω on $SE(2)$ is given by

$$\omega_g(X_g) = \sum_{i=1}^{3} \langle \mathrm{d}\mathcal{A}^i\big|_g, X_g \rangle A_i, \qquad X_g \in T_g(SE(2)), \tag{3.15}$$

where $\{\mathrm{d}\mathcal{A}^i\}_{i=1}^3$ is given by (3.4) and $A_i = \mathcal{A}_i|_e$, recall (3.3). It is a Cartan Ehresmann connection form on the *principal fiber bundle* $P = (SE(2), e, SE(2), \mathcal{L}(SE(2)))$, where $\pi(g) = e$, $R_g u = ug$, $u, g \in SE(2)$. Let Ad denote the adjoint action of $SE(2)$ on its own Lie-algebra $T_e(SE(2))$, i.e. $\mathrm{Ad}(g) = (R_{g^{-1}} L_g)_*$, i.e. the push-forward of conjugation. Then the adjoint representation of $SE(2)$ on the vector space $\mathcal{L}(SE(2))$ of left-invariant vector fields is given by

$$\widetilde{\mathrm{Ad}}(g) = \mathrm{d}\mathcal{R} \circ \mathrm{Ad}(g) \circ \omega. \tag{3.16}$$

This adjoint representation gives rise to the *associated vector bundle* $SE(2) \times_{\widetilde{\mathrm{Ad}}} \mathcal{L}(SE(2))$. The corresponding connection form on this vector bundle is given by

$$\tilde{\omega} = \mathcal{A}_2 \otimes \mathrm{d}\mathcal{A}^3 \wedge \mathrm{d}\mathcal{A}^1 + \mathcal{A}_3 \otimes \mathrm{d}\mathcal{A}^1 \wedge \mathrm{d}\mathcal{A}^2. \tag{3.17}$$

Then $\tilde{\omega}$ yields the following 3×3-matrix valued matrix 1-form

$$\tilde{\omega}_j^k(\cdot) := -\tilde{\omega}(\mathrm{d}\mathcal{A}^{\mathrm{k}}, \cdot, \mathcal{A}_{\mathrm{j}}) \qquad \mathrm{k}, \mathrm{j} = 1, 2, 3. \tag{3.18}$$

on the frame bundle, [36, p.353,p.359], where the sections are moving frames [36, p.354]. Let $\{\mu_k\}_{k=1}^3$ denote the sections in the tangent bundle $E := (SE(2), T(SE(2)))$ which coincide with the left-invariant vector fields $\{\mathcal{A}_k\}_{k=1}^3$. Then the matrix-valued 1-form (3.18) yields the Cartan connection[6] D on the tangent bundle $(SE(2), T(SE(2)))$ given by the covariant derivatives

$$\begin{aligned} D_{X|_{\gamma(t)}}(\mu(\gamma(t))) &:= D\mu(\gamma(t))(X|_{\gamma(t)}) \\ &= \sum_{k=1}^{3} \dot{a}^k(t)\mu_k(\gamma(t)) + \sum_{k=1}^{3} a^k(\gamma(t)) \sum_{j=1}^{3} \tilde{\omega}_k^j(X|_{\gamma(t)})\, \mu_j(\gamma(t)) \\ &= \sum_{k=1}^{3} \dot{a}^k(t)\mu_k(\gamma(t)) + \sum_{i,j=1}^{3} \dot{\gamma}^i(t)\, a^k(\gamma(t))\, \Gamma_{ik}^j\, \mu_j(\gamma(t)) \end{aligned} \tag{3.19}$$

with $\dot{a}^k(t) = \dot{\gamma}^i(t)\,(\mathcal{A}_i|_{\gamma(t)}\, a^k)$, for all tangent vectors $X|_{\gamma(t)} = \dot{\gamma}^i(t)\ \mathcal{A}_i|_{\gamma(t)}$ along a curve $t \mapsto \gamma(t) \in SE(2)$ and all sections $\mu(\gamma(t)) = \sum_{k=1}^{3} a^k(\gamma(t))\, \mu_k(\gamma(t))$. The Christoffel

[6]Following the definitions in [36], it is formally not right to call this the Cartan connection. It is the Koszul connection, [36, p.242] corresponding to the Cartan connection, [p.353][36], i.e. the associated differential operator corresponding to a Cartan connection. For a complete overview on Koszul connections, Ehresmann connections (the most general ones), Cartan connections and classical connections, see [36, p.386-387]. From now on we avoid all these technicalities and just use "Cartan connection" (a Koszul connection in [36]) and "Cartan-Ehresmann connection form" (Ehresmann connection in [36]).

symbols in (3.19) are constant $\Gamma^j_{ik} = -c^j_{ik}$, with c^j_{ik} the structure constants of Lie-algebra $T_e(SE(2))$. The curvature tensor equals

$$D^2 = R^j_{i,kl} \mathrm{d}\mathcal{A}^i \otimes \mathrm{d}\mathcal{A}^k \otimes \mathrm{d}\mathcal{A}^l \otimes \mathcal{A}_j = \mathcal{A}_2 \otimes \mathrm{d}\theta \otimes \mathrm{d}\theta \wedge \mathrm{d}\mathcal{A}^2 \ + \ \mathcal{A}_3 \otimes \mathrm{d}\theta \otimes \mathrm{d}\theta \wedge \mathrm{d}\mathcal{A}^3. \quad (3.20)$$

which arises from (3.9) by taking the limit $\beta \downarrow 0$. So the curvature on $SE(2)$ is constant, the sectional curvature of the planes spanned by respectively $\{\partial_\theta, \partial_\xi\}$ and by $\{\partial_\theta, \partial_\eta\}$ is constant$=1$, the sectional curvature of the plane spanned by $\{\partial_\xi, \partial_\eta\}$ vanishes.

Proof. For proof see Appendix B. □

The next theorem relates the previous results on Cartan connections and covariant derivatives to our non-linear diffusion schemes on $SE(2)$.

THEOREM 3.9. The covariant derivative of a co-vector field $\mathbf{a}$ on the manifold $((SE(2))^\beta, \mathcal{G}^\beta)$ is a (0,2)-tensor field with components: $\nabla_j a_i = \mathcal{A}_j a_i - \Gamma^k_{ji} a_k$, whereas the covariant derivative of a vector field $\mathbf{v}$ on $(SE(2))^\beta$ is a (1,1)-tensor field with components $\nabla_{j'} v^i = \mathcal{A}_{j'} v^i + \Gamma^i_{j'k'} v^{k'}$. Here the Christoffel symbols equal minus the structure-constants of the Lie-algebra $\mathcal{L}((SE(2))^\beta)$: $\Gamma^k_{ij} = -c^k_{ij}$ using short notation $\nabla_j := D_{\mathcal{A}_j}$, where D denotes the Cartan connection on $(SE(2))_\beta$. The Christoffel symbols are anti-symmetric as the underlying Cartan connection[7] D has constant *curvature* and constant *torsion*. The left-invariant evolution equations (1.9) can be rewritten in covariant derivatives:

$$\begin{cases} \partial_s W(g,s) = \sum\limits_{i,j=1}^{3} \mathcal{A}_i \left((D_{ij}(W))(g,s) \mathcal{A}_j W\right)(g,s) = \sum\limits_{i,j=1}^{3} \nabla_i \left((D_{ij}(W))(g,s) \nabla_j W\right)(g,s) \\ W(g,0) = \mathcal{W}_\psi f(g) \ , \qquad \text{for all } g \in SE(2), s>0. \end{cases} \quad (3.21)$$

Both convection and diffusion in the left-invariant evolution equations (1.9) take place along the exponential curves in $SE(2)$ which are the covariantly constant curves with respect to the Cartan connection. These curves are circular spirals in $\mathbb{R}^2 \times [0, 2\pi)$:

$$\begin{aligned} t \mapsto g_0 \, \exp(t(\sum_{i=1}^{3} c_i A_i)) &= (x_0 + \tfrac{c_3}{c_1}(\cos(c_1 t + \theta_0) - \cos\theta_0) + \tfrac{c_2}{c_1}(\sin(c_1 t + \theta_0) - \sin\theta_0), \\ & y_0 + \tfrac{c_3}{c_1}(\sin(c_1 t+\theta_0) - \sin\theta_0) - \tfrac{c_2}{c_1}(\cos(c_1 t+\theta_0) - \cos\theta_0), e^{i(c_1 t + \theta_0)}), \qquad c_1 \neq 0, \end{aligned} \quad (3.22)$$

for all $g_0 = (x_0, y_0, e^{i\theta_0}) \in SE(2)$, with radius $\frac{\sqrt{c_2^2+c_3^2}}{c_1}$ and central point $(-\frac{c_3}{c_1}\cos\theta_0 - \frac{c_2}{c_1}\sin\theta_0 + x_0, \frac{c_2}{c_1}\cos\theta_0 - \frac{c_3}{c_1}\sin\theta_0 + y_0)$. For $c_1 = 0$ the exponential curves are given by

$$t \mapsto g_0 \, \exp(t(c_2 A_2 + c_3 A_3)) = (x_0 + t\, c_2 \cos\theta_0 - t\, c_3 \sin\theta_0, y_0 + t\, c_2 \sin\theta_0 + t\, c_3 \cos\theta_0, e^{i\theta_0}).$$

Proof. The first part of the proof is a straightforward generalization of Theorem 3.8, where $\beta = 0$. Here we note that by Theorem 3.2 covariant differentiation takes place on a symmetric Riemannian manifolds $((SE(2))_\beta), \mathcal{G}_\beta$ iff $\beta > 0$. We know by Theorem 3.2 that the curvature of the Cartan connection D on $(SE(2))_\beta$ is constant. Now the torsion tensor $T(X,Y) = D_X Y - D_Y X - [X,Y]$ is constant as well, since $T[\mathcal{A}_i, \mathcal{A}_j] = D_{\mathcal{A}_i}\mathcal{A}_j - D_{\mathcal{A}_j}\mathcal{A}_i - [\mathcal{A}_i, \mathcal{A}_j] = \sum_k (\Gamma^k_{ij}\mathcal{A}_k - \Gamma^k_{ji}\mathcal{A}_k - c^k_{ij}\mathcal{A}_k) = -3\sum_k c^k_{ij}\mathcal{A}_k$. Finally, the covariant constant curves γ (or "auto-parallel" curves) are by definition given by $D_{\dot{\gamma}}\dot{\gamma} = 0$ on the tangent bundle $(SE(2), T(SE(2)))$:

$$D_{\dot{\gamma}}\dot{\gamma} = D_{\dot{\gamma}^i \mathcal{A}_i|_{\gamma(t)}} \dot{\gamma}^i \mathcal{A}_i|_{\gamma(t)} = \ddot{\gamma}^i \mathcal{A}_i|_{\gamma(t)} + \dot{\gamma}^i \dot{\gamma}^k \Gamma^j_{ik} \mathcal{A}_j = \ddot{\gamma}^i \mathcal{A}_i|_{\gamma(t)} = 0, \quad (3.23)$$

[7]Our Cartan connection is *not* related to a Levi-Civita connection (where Christoffels are symmetric).

where we again apply automatic summation over double indices and where $\Gamma^k_{ij} = -\Gamma^k_{ji} = c^k_{ji} = -c^k_{ij}$. Apparently, tangent vectors to auto-parallel curves have constant coefficients with respect to $\{\mathcal{A}_1, \mathcal{A}_2, \mathcal{A}_3\}$, i.e. $\forall_{t>0}\ \dot{\gamma}^i(t) = \langle \mathrm{d}\mathcal{A}^i\big|_{\gamma(t)}, \dot{\gamma}(t)\rangle = \langle \mathrm{d}\mathcal{A}^i\big|_{\gamma(0)}, \dot{\gamma}(0)\rangle = c^i \in \mathbb{R}, i = 1, 2, 3$. Now for $U : SE(2) \to \mathbb{C}$ smooth one has

$$
\begin{aligned}
&\tfrac{d}{dt} U(\gamma(t)) = \lim_{h\to 0} \tfrac{U(\gamma(t+h)-U(\gamma(t)))}{h} = (\mathrm{d}\mathcal{R}(\sum_{i=1}^{3} c^i A_i)U)(\gamma(t)) = \sum_{i=1}^{3} c^i (\mathrm{d}\mathcal{R}(A_i)U)(\gamma(t)) \\
&= \sum_{i=1}^{3} c^i\ \mathcal{A}_i U|_{\gamma(t)}\,, \text{ where } \gamma(t) = g_0 e^{t\sum_{i=1}^{3} c^i A_i}, \text{ recall } A_i = \mathcal{A}_i|_e\,.
\end{aligned}
\tag{3.24}
$$

so these curves $\gamma(t)$ coincide with the exponential curves in $SE(2)$, derived in [16], [12]. Now the connection D is a Koszul connection, [36, p.241] and therefore $\nabla_i(U\mathcal{A}_j)\ \phi = \nabla_i(U\nabla_j)\ \phi = U\nabla_i\nabla_j\phi + (\nabla_i U)\ \phi$ for all $U \in C^1(SE(2)$ and all smooth $\phi \in C^\infty(SE(2))$. Now set $U = D_{ij}(W)(\cdot, s)$ and $\phi = W(\cdot, s)$ for all $s > 0$ and use $D_{ij} = D_{ji}$ and $\Gamma^k_{ij} = -\Gamma^k_{ji}$ and take the sum over both indices i, j and the result (3.21) follows. □

REMARK 3.10. Circular spirals are the only curves with non-zero *constant curvature and torsion* in the flat space $\mathbb{R}^2 \times [0, 2\pi)$. A circular spiral is covariantly constant in $(SE(2), T(SE(2)))$ with respect to the Cartan connection with *constant curvature and torsion* iff the principal axis of the cilinder containing the spiral lies in θ-direction.

3.3. *Horizontal curves and principal fiber bundles .* There exists a natural relation between curves in the plane $\mathbb{R}^2$ and curves in $SE(2)$. For every C^1-curve $s \mapsto (x(s), y(s))$ one can construct a unique corresponding curve in $SE(2)$ by $s \mapsto (x(s), y(s), \theta(s) = \arg(x'(s) + i\, y'(s)))$. Such curves in $SE(2)$ we will call *horizontal curves*.

DEFINITION 3.11. A curve $s \mapsto \gamma(s) = (x(s), y(s), e^{i\theta(s)})$ in $SE(2)$ is called horizontal iff $\theta(s) = \arg(x'(s) + i\, y'(s))$. Then γ is called the lifted curve in $SE(2)$ of the curve $s \mapsto \mathbf{x}(s) = (x(s), y(s))$ in $\mathbb{R}^2$. A tangent vector in $X_g \in T_g(SE(2))$ is called horizontal if it is the tangent vector to some horizontal curve through g. A vector field X is called horizontal if X_g is horizontal for all $g \in SE(2)$.

We want to diffuse on orientation scores mainly along horizontal exponential curves, for practical motivation see [22]. To get the right intuition: Recall [18, Fig.1], where typically the mass of an orientation score is concentrated around a horizontal curve.

A smooth horizontal curve $\gamma = (\mathbf{x}, \theta)$ in $SE(2)$ can be parameterized by the arc-length $s > 0$ of its projection $\mathbf{x} = \mathbb{P}_{\mathbb{R}^2}\gamma$ on the spatial plane. Using this spatial arc-length parametrization it is clear from Definition 3.11 that along a horizontal curve $\gamma = (\mathbf{x}, e^{i\theta}) : \mathbb{R}^+ \to SE(2)$ one has

$$
\gamma = (\mathbf{x}, e^{i\theta}) \text{ is horizontal } \Rightarrow \kappa(s) = \dot{\theta}(s), \tag{3.25}
$$

where $\kappa(s) = \pm\|\ddot{\mathbf{x}}(s)\|_{\mathbb{R}^2}$, with $\|\cdot\|_{\mathbb{R}^2}$ the Euclidean norm on $\mathbb{R}^2$, is the curvature of the curve $s \mapsto \mathbf{x}(s) = \mathbb{P}_{\mathbb{R}^2}\gamma(s)$. Furthermore, a smooth curve $s \mapsto \gamma(s)$ is horizontal iff

$$
\dot{\gamma}(s) \in \operatorname{span}\{\,\mathbf{e}_\theta|_{\gamma(s)}\,, \mathbf{e}_\xi|_{\gamma(s)}\} \text{ for all } s > 0, \tag{3.26}
$$

Here we denote tangent vectors as $\mathbf{e}_\theta(s) = \mathbf{e}_\theta$, $\mathbf{e}_\xi(s) = \cos\theta(s)\mathbf{e}_x + \sin\theta(s)\mathbf{e}_y$, $\mathbf{e}_\eta(s) = -\sin\theta(s)\mathbf{e}_x + \cos\theta(s)\mathbf{e}_y$ as they are considered as tangent vectors to (classes of) curves, rather than considering tangent vectors a differential operators $\{\partial_\theta, \partial_\xi, \partial_\eta\}$ on locally defined smooth functions, although it boils down to the same thing, recall [18, fig.4].

By equality (3.26) and Definition 3.11 it follows that the horizontal part $\mathcal{H}_g \subset T_g(SE(2))$ of each tangent space $T_g(SE(2))$ is spanned by $\mathcal{H}_g = \{\partial_\theta|_g, \partial_\xi|_g\}$ and the space of horizontal left-invariant vector fields is spanned by $\{\partial_\theta, \partial_\xi\} = \{\mathcal{A}_1, \mathcal{A}_2\}$. However, a horizontal curve itself $s \mapsto \gamma(s) \in SE(2)$ can have components in all directions $\{\mathbf{e}_\theta, \mathbf{e}_\xi, \mathbf{e}_\eta\}$, in contrast to $\dot{\gamma}(s) \in T_{\gamma(s)}(SE(2))$. In fact a smooth curve γ given by

$$s \mapsto \gamma(s) = \xi(s)\mathbf{e}_\xi(s) + \eta(s)\mathbf{e}_\eta(s) + \theta(s)\mathbf{e}_\theta(s), \tag{3.27}$$

with $\gamma(s) = (x(s), e^{i\theta(s)}) \in SE(2)$ and $s > 0$ arc length of the projected curve $x = \mathbb{P}_{\mathbb{R}^2}\gamma$, is a horizontal curve in $SE(2)$ iff $\frac{d\eta}{ds} = -\xi\kappa$. Moreover, for such curves we have $\frac{d\xi}{ds} - \kappa\eta = \|\dot{x}(s)\| = 1$. This follows by differentiation of $s \mapsto \gamma(s)$ and observation (3.26):

$$\frac{d}{ds}(\xi(s)\mathbf{e}_\xi(s)+\eta(s)\mathbf{e}_\eta(s)+\theta(s)\mathbf{e}_\theta) = (\dot{\xi}(s)-\kappa(s)\eta(s))\mathbf{e}_\xi(s)+(\dot{\eta}(s)+\kappa(s)\xi(s))\mathbf{e}_\eta(s)+\dot{\theta}(s)\mathbf{e}_\theta. \tag{3.28}$$

Differentiating a smooth function $C : SE(2) \to \mathbb{R}$ along a horizontal curve γ yields

$$\begin{aligned} \tfrac{d}{ds}C(\gamma(s)) &= \langle C_\xi(\gamma(s))\mathrm{d}\mathcal{A}^2 + C_\eta(\gamma(s))\mathrm{d}\mathcal{A}^3 + C_\theta(\gamma(s))\mathrm{d}\theta, \dot{\gamma}(s)\rangle \\ &= \left(C_\xi(\gamma(s))\left(\tfrac{d\xi}{ds} - \kappa(s)\eta(s)\right) + C_\eta(\gamma(s))\left(\tfrac{d\eta}{ds} + \kappa(s)\xi(s)\right) + C_\theta(\gamma(s))\kappa(s)\right) \\ &= C_\xi(\gamma(s)) + \kappa(s)\, C_\theta(\gamma(s)) \ . \end{aligned} \tag{3.29}$$

A horizontal curve can be mapped to a new horizontal curve by right multiplication with a fixed element from the subgroup $Y = \{(0, y, e^{i0} = 1) \mid y \in \mathbb{R}\}$. Here we note that

$$\gamma(s)\,(0, y, 1) = (\mathbf{x}(s), e^{i\theta(s)})\,(0, y, 1) = (\mathbf{x}(s) + y\mathbf{e}_\eta(s), e^{i\theta(s)})$$

and $\dot{\mathbf{x}}^{NEW}(s) = \dot{\mathbf{x}}(s) + \frac{d}{ds}\mathbf{e}_\eta(s) = \dot{\mathbf{x}}(s) + \kappa(s)\mathbf{e}_\xi(s) = (1 + \kappa(s))\mathbf{e}_\xi(s)$, so again the horizontal condition $\theta^{NEW}(s) = \arg(\dot{x}^{NEW}(s) + i\dot{y}^{NEW}(s))$ holds and therefore

$$s \mapsto \gamma(s) \text{ is horizontal } \Rightarrow s \mapsto (\gamma(0, h, 0))(s) := \gamma(s)(0, h, 0) \text{ is horizontal} \ . \tag{3.30}$$

In fact Y is the only subgroup of $SE(2)$ which has this property, whereas left multiplication of a horizontal curve with any fixed element from $SE(2)$ always yields a horizontal curve again. For an overview of all (length preserving) perturbations of horizontal curves into horizontal curves see [17]app.C.

Let us return to our goal of diffusing on orientation scores along horizontal exponential curves, for practical motivation see [22]. Now by (3.26) this simply means that in the diffusion generator (1.8) of our non-linear diffusion system on orientation scores (3.21), all ∂_η derivatives should be removed (or equivalently set $a_3 = D_{i3} = D_{3i} = 0$, $i = 1, 2, 3$). Recall from [18] that this removal does not cause singular behavior (like it would on $\mathbb{R}^3$) iff $\{1, 3\} \in \{i \mid a_i \neq 0 \vee D_{ii} \neq 0\}$ or $\{1, 2\} \in \{i \mid a_i \neq 0 \vee D_{ii} \neq 0\}$, because of the non-commutativity of $SE(2)$ and Hörmander's condition. Here we stress that diffusion does not take place on an integrable $2D$ sub-manifold of $SE(2)$ (not even locally !), due to the non-integrability of the $\{\mathrm{d}\mathcal{A}^1, \mathrm{d}\mathcal{A}^2\} = \{\mathrm{d}\theta, \cos\theta\mathrm{d}x + \sin\theta\mathrm{d}y\}$-foliation. Nor does the horizontal diffusion take place on the quotient $SE(2)/Y$, as horizontal curves can have an η-component in (3.27).

Summarizing, we need a better mathematical grip on the removal of the third direction in the tangent space. Now technically speaking it means that diffusion takes place along the contact manifold $\{SE(2), \mathrm{d}\mathcal{A}^3\}$, [7, p.9]. Here we note that $\mathrm{d}\mathrm{d}\theta = 0$ and

$$\begin{aligned} \mathrm{d}(-\sin\theta\,\mathrm{d}x + \cos\theta\,\mathrm{d}y) &= -\cos\theta\,\mathrm{d}\theta \wedge \mathrm{d}x - \sin\theta\,\mathrm{d}\theta \wedge \mathrm{d}y, \\ \mathrm{d}(\cos\theta\,\mathrm{d}x + \sin\theta\,\mathrm{d}y) &= -\sin\theta\,\mathrm{d}\theta \wedge \mathrm{d}x + \cos\theta\,\mathrm{d}\theta \wedge \mathrm{d}y, \end{aligned} \tag{3.31}$$

which basicly is Cartan's structural formula on $SE(2)$, [1], (B.10), in explicit form. For example one has $\mathrm{d}\mathrm{d}\mathcal{A}^3 = -\mathrm{d}\mathcal{A}^1 \wedge \mathrm{d}\mathcal{A}^2$, where in the left-hand side only the left d denotes an exterior derivative ($\mathrm{d}\mathcal{A}^i$ denotes the dual vector to $\mathcal{A}_i$ as in Theorem 3.1). So the non-degeneracy condition on the Pfaffian form $\mathrm{d}\mathcal{A}^2$ of the contact manifold [7, p.9] is indeed satisfied : $\mathrm{d}\mathcal{A}^3 \wedge \mathrm{d}\mathrm{d}\mathcal{A}^3 = \mathrm{d}\mathcal{A}^1 \wedge \mathrm{d}\mathcal{A}^2 \wedge \mathrm{d}\mathcal{A}^3 \neq 0$. It is well-known in theory on contact manifolds [7] that the only integrable sub-manifolds are one dimensional and they are usually called *Legendre submanifolds*, which in our case simply coincide with *horizontal curves* on $SE(2)$. Contact manifold theory, [6] is highly useful for optimization of Lagrangians along horizontal curves, [7, ch:1.2], as can be seen in Appendix A. But it is mainly based on Pfaffian forms (elements in the dual tangent space) and we rather need a fiber structure in the *manifold* $SE(2)$. Therefor we will use the Pfaffian form $\mathrm{d}\mathcal{A}^3$ of the contact manifold in an Ehresmann connection of a principle fiber bundle on $SE(2)$. So we consider the domain of the (evolving) orientation score as the following principal fiber bundle

$$P_Y = (SE(2), SE(2)/Y, \pi, R), \tag{3.32}$$

with subgroup $Y = \{(0, y, e^{i0}) \,|\, y \in \mathbb{R}\}$, right-multiplication $R_h g = gh$, $h \in Y$, $g \in SE(2)$ and projection $\pi : SE(2) \to SE(2)/Y$ given by $\pi(g) = gY = \{g' \in SE(2) \mid g' \sim g \text{ i.e. } g^{-1}g' \in Y\}$, so that $\pi(gh) = \pi(g)$ for all $g \in SE(2)$, $h \in Y$. For more details on principal fiber bundles in general, see [28], [36], [34].

Here we stress that coordinate free differential geometry on principal fiber bundles starts with horizontal lifts as defined below. These horizontal lifts define parallel transport (which turns out to be independently on the choice of horizontal lift), [36, ch:8, p.365] and parallel transport defines the covariant derivative [36, p.366] which yields a connection[8], [36, p.367-368].

Definition 3.12. A horizontal lift of a curve $\gamma : [0,1] \to SE(2)/Y$ is a horizontal curve $\gamma^* : [0,1] \to SE(2)$ such that $\pi(\gamma^*) = \gamma$.

It can be shown [36, prop. 7, p.363] that for every curve in $\gamma : [0,1] \to SE(2)/Y$ with $\gamma(0) = g_0 Y$ for some $g_0 \in P_Y$ meaning $g_0 \in SE(2)$, say $\pi(g_0) = g_0 Y$ there exists a unique lift γ^* of γ such that $\gamma^*(0) = g_0$. In fact horizontal lifts are uniquely determined by right multiplication and since Y is the unique subgroup satisfying (3.30), we are able to relate our basic definition of horizontal vector fields, Definition 3.11, to the standard definition of horizontal vector fields on the principal fiber bundle P_Y, see Theorem 3.13.

On P_Y one can still impose a left-invariant metric $\mathcal{G}_\beta$, as is done in Theorem 3.13, again parameterized by the same $\beta > 0$, by removing left-invariant direction $\mathcal{A}_3$ from each tangent space. The geodesics on this principal fiber bundle are closely related to elastica curves and are derived in Appendix A. Our formula for these geodesics are much more tangible than the well-known formula for the corresponding elastica curves, [31], [6]. For a comparison between elastica and corresponding geodesics, see [17, Ch: 7, Fig.13].

Theorem 3.13. The set $P_Y = (SE(2), SE(2)/Y, \pi, R)$ with subgroup $Y = \{(0, y, e^{i0}) \mid y \in \mathbb{R}\}$, projection $\pi(g) = gY$ and right-multiplication $R_h g = gh$, $h \in Y$, is a principal fiber

[8]This Koszul connection coincides, [36, p.368-371], with the Koszul connection [p.320][36] obtained from the Cartan connection, [36, ch:7,p.314] corresponding to an Ehresmann connection, [36, p.359] on the frame-bundle $F(SE(2)/Y)$, [36, ch:7,p.345].

bundle (with structure group Y) on which $\omega = (L_{0,-y,0})_*$ is a Cartan-Ehresmann connection form and in the moving frame of reference $\{\mathcal{A}_1, \mathcal{A}_2, \mathcal{A}_3\}$ it is given by

$$\omega_g(X_g) = \langle \mathrm{d}\mathcal{A}^2\big|_g, X_g\rangle A_2 = \langle -\sin\theta\,\mathrm{d}x + \cos\theta\,\mathrm{d}y, X_g\rangle \partial_y \ , \qquad X \in \mathcal{L}(SE(2)). \quad (3.33)$$

The horizontal part $\mathcal{H}_g$ of each tangent space $T_g(SE(2))$, $g \in SE(2)$ is by definition

$$\mathcal{H}_g := \ker\{\omega_g\} = \mathrm{span}\,\{\,\mathcal{A}_1|_g\,,\, \mathcal{A}_2|_g\} = \mathrm{span}\,\{\partial_\theta, \cos\theta\,\partial_x + \sin\theta\partial_y\} \qquad (3.34)$$

and it coincides with the vector space space of tangent vectors along all possible horizontal curves passing through $g \in SE(2)$, recall Definition 3.11. The connection form $\tilde{\omega}$ on the associated vector bundle $SE(2) \times_{\widetilde{\mathrm{Ad}}} \mathcal{L}(SE(2))$ is given by

$$\tilde{\omega} = -\mathcal{A}_2 \otimes \mathrm{d}\mathcal{A}^1 \otimes \mathrm{d}\mathcal{A}^3 = -(\cos\theta\,\partial_x + \sin\theta\,\partial_y) \otimes \mathrm{d}\theta \otimes (-\sin\theta\,\mathrm{d}x + \cos\theta\,\mathrm{d}y). \quad (3.35)$$

The *horizontal auto-parallels* of connection $D = d + \overline{\omega}$, with $\overline{\omega}(a^k\mathcal{A}_k) = -a^k\tilde{\omega}(\mathrm{d}\mathcal{A}^j, \cdot, \mathcal{A}_k)\mathcal{A}_j$,

$$D_{a^i\mathcal{A}_i}(\dot{\gamma}^i\ \mathcal{A}_i|_{\gamma(t)}) = (D\,a^i\mathcal{A}_i)(\dot{\gamma}^i\ \mathcal{A}_i|_{\gamma(t)}) = \dot{a}^1\ \mathcal{A}_1|_{\gamma(t)} + (\dot{a}^2 + a^3\dot{\gamma}^1)\ \mathcal{A}_2|_{\gamma(t)} + \dot{a}^3\ \mathcal{A}_3|_{\gamma(t)}\,, \quad (3.36)$$

are the *horizontal exponential curves*, given by (3.22) with $c_3 = 0$, see Figure 5.

Finally, we equip P_Y with the following left-invariant form

$$\mathcal{G}_\beta = \mathrm{d}\theta \otimes \mathrm{d}\theta + \beta^2 \mathrm{d}\mathcal{A}^2 \otimes \mathrm{d}\mathcal{A}^2, \qquad (3.37)$$

which yields a left-invariant metric on $SE(2)$: $d_{SE(2)}(g, g_0) = d_{SE(2)}(g_0^{-1}g, e)$ defined by

$$\begin{aligned} d_{SE(2)}(g_0^{-1}g, e) &= \inf\{\int_0^1 \sqrt{(\theta'(t))^2 + \beta^2\|\mathbf{x}'(t)\|^2}\,\mathrm{d}t \,|\, \gamma \text{ horizontal}, \gamma(0) = e, \gamma(L) = g_0^{-1}g\} \\ &= \inf\{\int_0^L \sqrt{(\kappa(s))^2 + \beta^2}\ \mathrm{d}s = \int_0^L \sqrt{g_{ij}\dot{\gamma}^i(s)\dot{\gamma}^j(s)}\mathrm{d}s \,|\, \gamma \text{ horizontal}, \gamma(0) = e, \gamma(L) = g_0^{-1}g\} \end{aligned} \qquad (3.38)$$

where $s > 0$ denotes the spatial arc-length parameter of the projected curve $\mathbf{x} = \mathbb{P}_{\mathbb{R}^2}\gamma$, with curvature $\kappa(s) = \|\ddot{\mathbf{x}}(s)\|$ in $\mathbb{R}^2$ and where $\dot{\gamma}^i(s) = \langle \mathrm{d}\mathcal{A}^i, \dot{\gamma}(s)\rangle$, $i = 1, 2, 3$. The explicit curves which minimize (3.38) are explicitly derived in Appendix A. In contrast to previous belief, [9], they do not exactly coincide with elastica curves, [31],[6].

Proof. The first part of the proof is analogue to the proof of Theorem 3.8 in Appendix B. The big difference though, is that instead of principal fiber bundle P with structure group $SE(2)$ we now have fiber bundle P_Y with structure group Y. In particular the base manifold $\{e\} \equiv SE(2)/SE(2)$ is now replaced by $SE(2)/Y$. In Theorem 3.8 every tangent vector is vertical, whereas in this theorem we are rather interested in the horizontal part $\mathcal{H}_g$ of the tangent space $T(SE(2)$. Note that by (3.26) the differential geometrical definition of horizontality $\mathcal{H}_g := \ker\{\omega_g\}$ coincides with the horizontality condition, Definition 3.11, required in the application ! The connection form ω_g is indeed a Cartan-Ehresmann connection form on P_Y: The first condition in Definition 3.6 is satisfied since $\omega \circ \mathrm{d}\mathcal{R}(A_3) = \omega(\mathcal{A}_3) = A_3$ and the second condition follows by (B.3) (special case $g \in Y$).

Again the Cartan connection D is obtained via the connection form $\tilde{\omega}$. This is the corresponding connection-form on the associated vector bundle $SE(2) \times_{\widetilde{\mathrm{Ad}}} \mathcal{L}(SE(2))$ given by $\tilde{\omega} = \widetilde{\mathrm{Ad}}_*(A_3) \otimes \mathrm{d}\mathcal{A}^3 = \widetilde{\mathrm{ad}}(A_3) \otimes \mathrm{d}\mathcal{A}^3 = c^k_{i3}\mathcal{A}_k \otimes \mathrm{d}\mathcal{A}^i \otimes \mathrm{d}\mathcal{A}^3 = c^2_{13}\mathcal{A}_2 \otimes \mathrm{d}\mathcal{A}^1 \otimes \mathrm{d}\mathcal{A}^3$, yielding (3.35). Here we note that direct computation yields $\overline{\omega}(a^1\mathcal{A}_1 + a^2\mathcal{A}_2 + a^3\mathcal{A}_3) = a^3\mathrm{d}\mathcal{A}^1(\,\cdot\,)\mathcal{A}_2$ from which (3.36) directly follows. Tangent vectors $\dot{\gamma} = \sum_i \dot{\gamma}^i(t)\ \mathcal{A}_i|_{\gamma(t)}$ to auto-parallel curves satisfy; $\nabla_{\dot{\gamma}}\dot{\gamma} = 0 \Leftrightarrow \ddot{\gamma}^2 = -\dot{\gamma}^1\dot{\gamma}^3$ and $\ddot{\gamma}^1 = \ddot{\gamma}^3 = 0$, so in particular if they are horizontal we find $\ddot{\gamma}^2 = \ddot{\gamma}^1 = \dot{\gamma}^3 = 0$. As a result all auto-parallel curves in the fiber bundle are horizontal exponential curves (3.22) with *constants* $c_1 = \dot{\gamma}^1$, $c_2 = \dot{\gamma}^2$, $c_3 = 0$. Now (3.37) follows from (3.13) by omitting the vertical direction $\mathcal{A}_3$ and in (3.38) we stress that the Lagrangian is parameter independent, so we may as well choose the spatial arc length-parameter $s > 0$ of the projection of the horizontal curve on the spatial plane with length L, in which case we have $\kappa(s) = \dot{\theta}(s)$. The metric (3.37) coincides with the metric in [9] (where this metric is called elastica functional) and is related to the well-known elastica functional $\int_0^L \kappa^2(s) + \beta^2 \mathrm{d}s$, [31],[6], for curves in $\mathbb{R}^2$. The important difference though is the square root ! This square root ensures that the functional is parameter independent in $SE(2)$, whereas the elastica functional is only parameter independent on $\mathbb{R}^2$. In a standard Riemannian manifold it does not matter if one applies a monotonic transformation on the integrand of the metric (this monotonic transformation can be taken into account by a re-parametrization of the same curve). However this argument does not apply here since only for the spatial arclength-parametrization of a horizontal curve we have $\kappa(s) = \dot{\theta}(s)$. $\square$

Finally we note with respect to the fundamental parameter β^2, which in case of elastica denotes the typical fraction of bending and stretching energy, that there exist two fundamentally different approaches to relate minimal energy curves (to direct products of Green's functions) of stochastic processes on $SE(2)$ with linear forward Kolmogorov equations, parameterized by constants $\alpha > 0$, $[D_{ij}] \geq 0$ as considered in part I [18]. If one follows the approach by Mumford, [31] to relate elastica curves to the direction process (a contour completion process) one must set $\beta^2 = 4\alpha D_{11}$, if one follows Brownian bridge theory, [17, app.B] to relate geodesics to a contour enhancement process with $D_{ij} \neq 0 \Leftrightarrow (i = j = 1 \text{ or } i = j = 2)$ one takes the limit $\alpha^{-1} \to 0$ and sets $\beta^2 = D_{11}/D_{22}$.

3.4. *Extraction of spatial curvature from orientation scores* . Let $U : SE(2) \to \mathbb{R}^+$ be some positive smooth function on $SE(2)$. This could for example be the absolute value $U = |\mathcal{W}_\psi f| = \sqrt{(\Re(\mathcal{W}_\psi f))^2 + (\Im(\mathcal{W}_\psi f))^2}$ of a (processed) orientation score of an image, which is positive and phase invariant, see part I [18, fig.3]. Then the exponential curves through g_0 with direction $c^i\ \mathcal{A}_i U|_{g_0}$ form "tangent spirals" (where we naturally embed $SE(2)$ into $\mathbb{R}^2 \times [-\pi, \pi)$) to the orientation score $\mathcal{W}_\psi f : SE(2) \to \mathbb{R}^+$. In particular, the horizontal exponential curves are given by (3.22). See Figure 5. In this section we will provide fast algorithms for curvature estimation at each $g_0 \in SE(2)$ in the domain of U, by finding the exponential curve through g_0 that fits U locally in an optimal way.

Remark 3.14. Sometimes we restrict ourselves to horizontal exponential curve fits, however, orientation scores $\mathcal{W}_\psi f$ and their absolute value $U = |\mathcal{W}_\psi f|$ in general do not satisfy $\partial_\eta U = 0$. So from a strict point of view this restriction is not entirely appropriate. Nevertheless, the density $U = |\mathcal{W}_\psi f|$ is typically concentrated around horizontal curves. Recall for example Figure 1 in Part I of this article.

For the exact definition of such an optimally fitting (horizontal) tangent spiral we first need a few preliminaries.

We apply the left-invariant first fundamental form (3.13) on $T(SE(2)) \times T(SE(2))$. Then the norm of a left-invariant vector field $c^i \mathcal{A}_i$ equals

$$|c^i \mathcal{A}_i|_\beta = \sqrt{(c^i \mathcal{A}_i, c^i \mathcal{A}_i)_\beta} = \sqrt{(c^\theta)^2 + (\beta\, c^\xi)^2 + (\beta\, c^\eta)^2} =: \|\mathbf{c}\|_\beta, \tag{3.39}$$

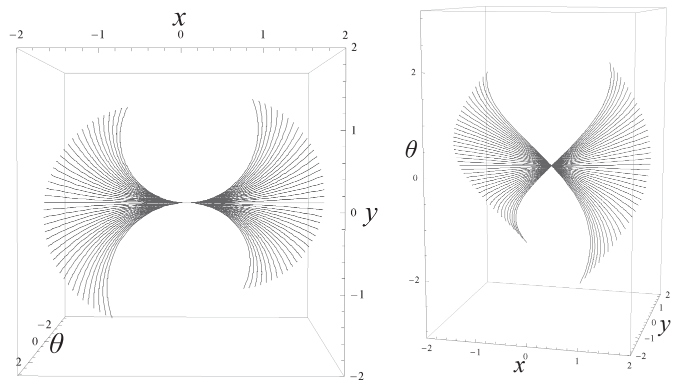

FIG. 5. All horizontal exponential curves through a fixed point $g \in SE(2)$ for different curvature values, shown from 2 different viewpoints. The left image shows that these curves correspond to circular arcs if projected onto te spatial plane. These curves coincide with the auto-parallels, see (3.22), in the principal fiber bundle P_Y.

with $\mathbf{c} = (c^1, c^2, c^3) \in \mathbb{R}^3$. Here we stress that the norm $|\cdot|_\beta : \mathcal{L}(SE(2)) \to \mathbb{R}^+$ is defined on the space $\mathcal{L}(SE(2))$ of left-invariant vector fields on $SE(2)$, whereas the norm $\|\cdot\|_\beta : \mathbb{R}^3 \to \mathbb{R}^+$ is defined on $\mathbb{R}^3$. The gradient $\mathrm{d}U$ of $U : SE(2) \to \mathbb{R}^+$ is given by $\mathrm{d}U = \frac{\partial U}{\partial \theta}\mathrm{d}\theta + \frac{\partial U}{\partial \xi}\mathrm{d}\mathcal{A}^2 + \frac{\partial U}{\partial \eta}\mathrm{d}\mathcal{A}^3$. The corresponding vector field equals $\mathcal{G}^{-1}\mathrm{dU} = \frac{\partial U}{\partial \theta}\partial_\theta + \beta^{-2}\frac{\partial U}{\partial \xi}\partial_\xi + \beta^{-2}\frac{\partial U}{\partial \eta}\partial_\eta$. Note that $\mathcal{G}^{-1}\mathrm{d}\mathcal{A}^k = g^{ki}\mathcal{A}_i$, with $g^{ij}g_{jl} = \delta^i_l$.

The norm of a co-vector field (such as the gradient $\mathrm{d}U$) is given by

$$|a_i \mathrm{d}A^i|^2_\beta = g^{ij}a_i a_j = (a_\theta)^2 + \beta^{-2}(a_\xi)^2 + \beta^{-2}(a_\eta)^2 = \|\mathbf{a}\|_{\beta^{-1}} \text{ with } \mathbf{a} = (a^1, a^2, a^3).$$

If we differentiate a smooth function $U : SE(2) \to \mathbb{R}^+$ along an exponential curve $\gamma(t) = g_0 \exp(t(\sum c^i A_i))$ passing g_0 we get, recall (3.24),

$$\frac{d}{dt}U(\gamma(t)) = \sum_{i=1}^3 c^i\, \mathcal{A}_i U|_{\gamma(t)} = c^1\, U_\theta(\gamma(t)) + c^2\, U_\xi(\gamma(t)) + c^3\, U_\eta(\gamma(t)). \tag{3.40}$$

After these preliminaries we return to our goal of finding the optimal tangent spiral at position $g_0 \in SE(2)$ given $U : SE(2) \to \mathbb{R}^+$.

DEFINITION 3.15. Consider the solution of the following minimization problem

$$\mathbf{c}_* = \arg \min_{\{c^i\}_{i=1}^3} \left\{ \left| \frac{d}{dt}\, \mathrm{d}U(\gamma(t))\Big|_{t=0} \right|^2_\beta \mid \gamma(t) = g_0 \exp(t(\sum_{i=1}^3 c^i A_i))\ ;\ \|\mathbf{c}\|_\beta = 1 \right\}. \tag{3.41}$$

Then we call the covariantly constant curve $t \mapsto g_0 e^{t \sum_{i=1}^3 c^i_* A_i}$ the optimal tangent spiral at $g_0 \in SE(2)$ given $U : SE(2) \to \mathbb{R}^+$.

By means of (3.40) and the chain rule the energy in (3.41) can be rewritten as

$$\begin{aligned} &\left| \tfrac{d}{dt}(\mathrm{d}U)(\gamma(t))\big|_{t=0} \right|^2_\beta = \left\| \nabla(\nabla U)^T(\gamma(0)) \cdot \gamma'(0) \right\|^2_{\beta^{-1}} \\ &= \left\| \left(\begin{array}{ccc} \partial_\theta(\partial_\theta U) & \partial_\xi(\partial_\theta U) & \partial_\eta(\partial_\theta U) \\ \partial_\theta(\partial_\xi U) & \partial_\xi(\partial_\xi U) & \partial_\eta(\partial_\xi U) \\ \partial_\theta(\partial_\eta U) & \partial_\xi(\partial_\eta U) & \partial_\eta(\partial_\eta U) \end{array} \right)\Bigg|_{g_0} \left(\begin{array}{c} c^1 \\ c^2 \\ c^3 \end{array} \right) \right\|^2_{\beta^{-1}} =: \|\, HU|_{g_0}\, \mathbf{c}\|^2_{\beta^{-1}}, \end{aligned} \tag{3.42}$$

where $\nabla U := (\partial_\theta U, \partial_\xi U, \partial_\eta U)$ and where the non-covariant Hessian HU does *not* coincide with the covariant Hessian form consisting of covariant derivatives of the Cartan connection, which we provided in Theorem 3.9. The covariant Hessian form is:

$$\begin{aligned}[\nabla_i \nabla_j U] &= [\nabla_i \mathcal{A}_j U] = [\mathcal{A}_i \mathcal{A}_j U + \Gamma^{\lambda}_{ij}\, \mathcal{A}_\lambda U] \\ &= \begin{pmatrix} \partial_\theta(\partial_\theta U) & \partial_\theta(\partial_\xi U) & \partial_\theta(\partial_\eta U) \\ \partial_\xi(\partial_\theta U) & \partial_\xi(\partial_\xi U) & \partial_\xi(\partial_\eta U) \\ \partial_\eta(\partial_\theta U) & \partial_\eta(\partial_\xi U) & \partial_\eta(\partial_\eta U) \end{pmatrix}.\end{aligned} \tag{3.43}$$

For example on 2nd row and 1st column we have $\nabla_1 \nabla_2 U = (\partial_\theta \partial_\xi - c^3_{12} \partial_\eta)U = \partial_\xi(\partial_\theta U)$. Note that the minimization problem (3.41) can now be rewritten as

$$\arg\min_{\mathbf{c}} \left\{ \|(HU)(g_0)\, \mathbf{c}\|^2_{\beta^{-1}} \mid \|\mathbf{c}\|_\beta = 1 \right\}.$$

Set $M_\beta := \mathrm{diag}\{1, \beta^{-1}, \beta^{-1}\} \in GL(3,\mathbb{R})$ and $H_\beta U := M_\beta\, HU\, M_\beta$ then by the Euler-Lagrange theory the gradient of $\|(HU)\mathbf{c}\|^2_{\beta^{-1}} = (\mathbf{c}, (HU)^T M^2_\beta (HU)\mathbf{c})_1$ at the optimum $\mathbf{c}_*$ is linearly dependent on the gradient of the side-condition, which can be written $(1 - \|\mathbf{c}\|^2_\beta) = 1 - (\mathbf{c}, M^{-2}_\beta \mathbf{c})_1 = 0$;

$$(HU(g_0))^T M^2_\beta (HU(g_0))\mathbf{c}_* = \lambda\, M^{-2}_\beta \mathbf{c}_* \;\Leftrightarrow\; (H_\beta U)^T (H_\beta U)\tilde{\mathbf{c}} = \lambda\, \tilde{\mathbf{c}},$$

for some Lagrange multiplier $\lambda \in \mathbb{R}$, where $\tilde{\mathbf{c}} = M^{-1}_\beta \mathbf{c}_*$.

So we have shown that the minimization problem (3.41) requires eigensystem analysis of $(H_\beta U)^T H_\beta U$, which is the product of the Hessian $H_\beta U$ and the covariant Hessian given by (3.43), which equals $(H_\beta U)^T$. The covariant Hessian also appears in the Euler-Lagrange equation for the following minimization problem (for simplicity we set $\beta = 1$)

$$\arg\min_{c^i} \left\{ \left| \frac{d^2}{dt^2} U(\gamma(t)) \right| \mid \gamma(t) = g_0 \exp(t(\sum_{i=1}^{3} c^i A_i))\ ;\ \|\mathbf{c}\|_{\beta=1} = 1 \right\}, \tag{3.44}$$

which by means of double application of (3.40) can be rewritten as

$$\left|\tfrac{d^2}{dt^2} U(\gamma(t))\right| = \left|\tfrac{d}{dt} c^i \mathcal{A}_i U(\gamma(t))\right| = \left|c^j c^i \mathcal{A}_j (\mathcal{A}_i U)(\gamma(t))\right| = \mid \mathbf{c}^T (\tfrac{1}{2}\ (HU + (HU)^T)\big|_{\gamma(t)})\mathbf{c} \mid$$

and as a result the Euler-Lagrange equations for the minimization problem (3.44) correspond to the eigensystem of $\frac{1}{2}(HU + (HU)^T)$: $\nabla \nabla^T U \mathbf{c} = \frac{1}{2}(HU + (HU)^T)\mathbf{c} = \lambda \mathbf{c}$.

Experiments on images consisting of lines with ground truth curvatures show that minimization problem (3.41) is preferable over (3.44) for spatial curvature estimation.

REMARK 3.16. On the commutative group $\mathbb{R}^2$ (i.e. the domain of images f rather than the domain of the orientation scores $\mathcal{W}_\psi f$) we do not have the difference between the two Hessians above, since here the Hessian $Hf = \begin{pmatrix} f_{xx} & f_{xy} \\ f_{yx} & f_{yy} \end{pmatrix}$ is square symmetric and thereby $Hf = \frac{1}{2}(Hf + (Hf)^T)$ and $(Hf)^T(Hf)$ have the same eigenvectors with respective eigenvalues $\{\lambda_n\}$ and $\{(\lambda_n)^2\}$.

We suggest the following 2 methods for curvature estimation. In the first approach we do not restrict ourselves to horizontal exponential curves, whereas in the second approach we enforce horizontality and obtain a horizontal curvature estimate.

1. Compute the curvature of the projection $\mathbf{x}(s(t)) = \mathbb{P}_{\mathbb{R}^2}\left(g_0 \exp(t(\sum_{i=1}^3 c^i_* A_i))\right)$ of the optimal exponential curve in $SE(2)$ on the ground plane from an eigenvector $\mathbf{c}_* =$

$(c_*^\theta, c_*^\xi, c_*^\eta)$. This eigenvector of $(\tilde{H}_\beta|U|)^T(\tilde{H}_\beta|U|)$, with 3×3-Hessian

$$\tilde{H}_\beta|U| = \begin{pmatrix} \beta^2\partial_\theta\partial_\theta|U| & \beta\partial_\xi\partial_\theta|U| & \beta\partial_\eta\partial_\theta|U| \\ \beta\partial_\theta\partial_\xi|U| & \partial_\xi\partial_\xi|U| & \partial_\eta\partial_\xi|U| \\ \beta\partial_\theta\partial_\eta|U| & \partial_\xi\partial_\eta|U| & \partial_\eta\partial_\eta|U| \end{pmatrix}, \tag{3.45}$$

is the one with smallest eigenvalue. The curvature estimation is now given by

$$\kappa_{est} = \|\ddot{\mathbf{x}}(s)\|\mathrm{sign}(\ddot{\mathbf{x}}(s)\cdot\mathbf{e}_\eta) = \frac{c_*^\theta \mathrm{sign}(c_*^\xi)}{\sqrt{(c_*^\xi)^2+(c_*^\eta)^2}}. \tag{3.46}$$

2. Compute the eigenvectors of $(\tilde{H}_\beta^{hor}|U|)^T(\tilde{H}_\beta^{hor}|U|)$ with horizontal Hessian

$$\tilde{H}_\beta^{hor}|U| = \begin{pmatrix} \beta^2\partial_\theta\partial_\theta|U| & \beta\partial_\xi\partial_\theta|U| \\ \beta\partial_\theta\partial_\xi|U| & \partial_\xi\partial_\xi|U| \\ \beta\partial_\theta\partial_\eta|U| & \partial_\xi\partial_\eta|U| \end{pmatrix} \tag{3.47}$$

to this end we recall that the optimum $\mathbf{c}_* = \arg\min\{\|\tilde{H}_\beta^{hor}|U|(g_0)\,\mathbf{c}\|^2_{\beta^{-1}} \mid \|\mathbf{c}\|_\beta = 1\}$ with $\mathbf{c} = (c^\theta, c^\xi) = c^\theta\mathbf{e}_\theta + c^\xi\mathbf{e}_\xi$ satisfies $2(\tilde{H}_\beta^{hor}|U|)^T\tilde{H}_\beta^{hor}|U|\,\tilde{\mathbf{c}} = 2\lambda\tilde{\mathbf{c}}$, $\mathbf{c}_* = M_\beta\tilde{\mathbf{c}}$ for some Lagrange multiplier λ. Then we compute the curvature of the projection $\mathbf{x}(s(t)) = \mathbb{P}_{\mathbb{R}^2}(g_0\exp(t(\sum c_*^i A_i)))$ of the exponential curve in $SE(2)$ on the ground plane from the eigenvector $\mathbf{c}_* = (c_*^\theta, c_*^\xi)$ with smallest eigenvalue:

$$\kappa_{est}^{hor} = \|\ddot{\mathbf{x}}(s)\|\mathrm{sign}(\ddot{\mathbf{x}}(s)\cdot\mathbf{e}_\eta) = \frac{c_*^\theta}{c_*^\xi} \tag{3.48}$$

For numerical experiments on the proposed curvature estimation (comparing the two methods above and the approach by van Ginkel [40]) on orientation scores of noisy example images, see [22], [21], [17].

4. Coherence Enhancing Diffusion on Orientation Scores . In order to obtain adaptive diffusion on orientation scores we will use the following basic nonlinear left-invariant evolution equations on $SE(2)$ as a starting point

$$\begin{cases} \partial_t U(g,t) = (\ \beta\partial_\theta\ \ \partial_\xi\ \ \partial_\eta\ ) \begin{pmatrix} (D_{11}(U))(g,t) & 0 & 0 \\ 0 & (D_{22}(U))(g,t) & 0 \\ 0 & 0 & (D_{33}(U))(g,t) \end{pmatrix} \begin{pmatrix} \beta\partial_\theta \\ \partial_\xi \\ \partial_\eta \end{pmatrix} U(g,t), \\ \text{for all } g\in SE(2), t>0, \\ U(g,t=0) = \mathcal{W}_\psi[f](g) \text{ for all } g\in SE(2), \end{cases} \tag{4.1}$$

with $\beta > 0$ (recall 3.8) and where the positive functions $D_{kk} : \mathbb{L}_2(SE(2)\times\mathbb{R}^+)\cap C^2(SE(2)\times\mathbb{R}^+) \to C^1(SE(2)\times\mathbb{R}^+)$, $k=1,2,3$ are given by

$$(g,t)\mapsto (D_{kk}(U))(g,t)\geq 0, \qquad U\in\mathbb{L}_2(SE(2)\times\mathbb{R}^+)\ .$$

These functions D_{kk}, $k=1,2,3$ should be chosen dependent on the local Hessian $HU(\cdot,t)$ of $U(\cdot,t)$ such that at strong orientations D_{33} should be small so that we have anisotropic diffusion in the spatial plane along the preferred direction ∂_ξ, while at weak directions D_{33} and D_{22} should be relatively large and isotropic $D_{22}\approx D_{33}$.

Example :

In the nonlinear diffusion system (4.1) we propose to set $D_{22}(U)(g,t) = 1$, $D_{11}(U)(g,t) =$

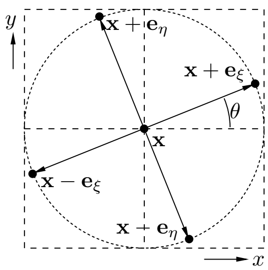

$$\partial_\theta u \approx \frac{1}{2s_\theta}\left(u(\mathbf{x}, l+1) - u(\mathbf{x}, l-1)\right)$$
$$\partial_\theta^2 u \approx \frac{1}{s_\theta^2}\left(u(\mathbf{x}, l+1) - 2u(\mathbf{x}, l) + u(\mathbf{x}, l-1)\right)$$
$$\partial_\xi u \approx \frac{1}{2}\left(u(\mathbf{x}+\mathbf{e}_\xi^l, l) - u(\mathbf{x}-\mathbf{e}_\xi^l, l)\right)$$
$$\partial_\xi^2 u \approx u(\mathbf{x}+\mathbf{e}_\xi^l, l) - 2u(\mathbf{x}, l) + u(\mathbf{x}-\mathbf{e}_\xi^l, l)$$
$$\partial_\eta u \approx \frac{1}{2}\left(u(\mathbf{x}+\mathbf{e}_\eta^l, l) - u(\mathbf{x}-\mathbf{e}_\eta^l, l)\right)$$
$$\partial_\eta^2 u \approx u(\mathbf{x}+\mathbf{e}_\eta^l, l) - 2u(\mathbf{x}, l) + u(\mathbf{x}-\mathbf{e}_\eta^l, l)$$
$$\partial_\xi\partial_\theta u \approx \frac{1}{4s_\theta}\left(u(\mathbf{x}+\mathbf{e}_\xi^l, l+1) - u(\mathbf{x}+\mathbf{e}_\xi^l, l-1) - u(\mathbf{x}-\mathbf{e}_\xi^l, l+1) + u(\mathbf{x}-\mathbf{e}_\xi^l, l-1)\right)$$
$$\partial_\theta\partial_\xi u \approx \frac{1}{4s_\theta}\left(u(\mathbf{x}+\mathbf{e}_\xi^{l+1}, l+1) - u(\mathbf{x}+\mathbf{e}_\xi^{l+1}, l-1) - u(\mathbf{x}-\mathbf{e}_\xi^{l-1}, l+1) + u(\mathbf{x}-\mathbf{e}_\xi^{l-1}, l-1)\right)$$

FIG. 6. Finite difference scheme of (4.1) where we use second order B-spline interpolation, [39], for sampling on the grid of our moving frame $\{\mathbf{e}_\theta, \mathbf{e}_\xi = \cos\theta\, \mathbf{e}_x + \sin\theta\, \mathbf{e}_y, \mathbf{e}_\eta = -\sin\theta\, \mathbf{e}_x + \cos\theta\, \mathbf{e}_y\}$.

$D_{33}(U)(g,t) = e^{-\frac{(s(|U|)(g,t))^2}{c}}$, where $c > 0$ is a standard non-linear diffusion parameter and where orientation confidence $s(U)(g,t)$ is given by

$$s(U)(g,t) = \max\{-(\partial_\eta^2 |U(g,t)| + \beta^2 \partial_\theta^2 |U(g,t)|),\ 0\}. \tag{4.2}$$

With respect to the numerics of (4.1) (and later (4.4)), we implemented a forward finite difference scheme using central differences along the moving frame $\{\theta, \xi, \eta\}$ where we used 2nd order B-spline interpolation, [39], to get the equidistant samples on the $\{\xi, \eta, \theta\}$-grid from the given samples on the $\{x, y, \theta\}$-grid, see figure 6. Our method is second order accurate on $SE(2)$ and only first order accurate in time. With this respect we note that a Crank-Nickolson scheme for time integration is second order in time and can improve computation time since one can take larger time steps. For comparison between coherence enhancing diffusions on images and orientation scores, see Figure 7.

4.1. *Including adaptive curvatures in the diffusion scheme by gauge-coordinates* . In subsection 3.4 we discussed two methods of how to obtain curvature estimates in orientation scores. This was done by finding the best exponential curve fit to the absolute value[9] $|\mathcal{W}_\psi f| : SE(2) \to \mathbb{R}^+$ of the orientation score $\mathcal{W}_\psi f : SE(2) \to \mathbb{C}$. We distinguished between two approaches. In the first approach (3.46) we consider the best exponential curve fit to the absolute value of the orientation score, whereas in the second approach we consider the best *horizontal* exponential curve fit to the absolute value of an orientation score (3.48). Both approaches yield a curvature estimate which in this paragraph we assume to be given. We shall write $\kappa := (\kappa_{est}(|U|))(g,t)$ for the curvature estimate of the score U via its absolute value $|U|$ at location $g \in SE(2)$ at time $t > 0$.

Now we can include curvature in our scheme (4.1) by replacing $\partial_\xi \mapsto \partial_\xi + \kappa\partial_\theta$. To this end we recall from Theorem 3.9 that the exponential curve $s \mapsto g_0\, e^{s\,(\partial_\xi + \kappa\partial_\theta)|_e} = g_0 e^{s(\partial_x + \kappa\partial_\theta)}$ yields a circular spiral (3.22) whose projection on $\mathbb{R}^2$ is a circle with radius

[9]The absolute value $|\mathcal{W}_\psi f|$ is phase invariant, recall Fig.3 in Part I of this article. This phase invariance is important for local feature estimation. Curvature estimation at the vicinity or border of a (thick) line should be similar to the estimate on top of the line.

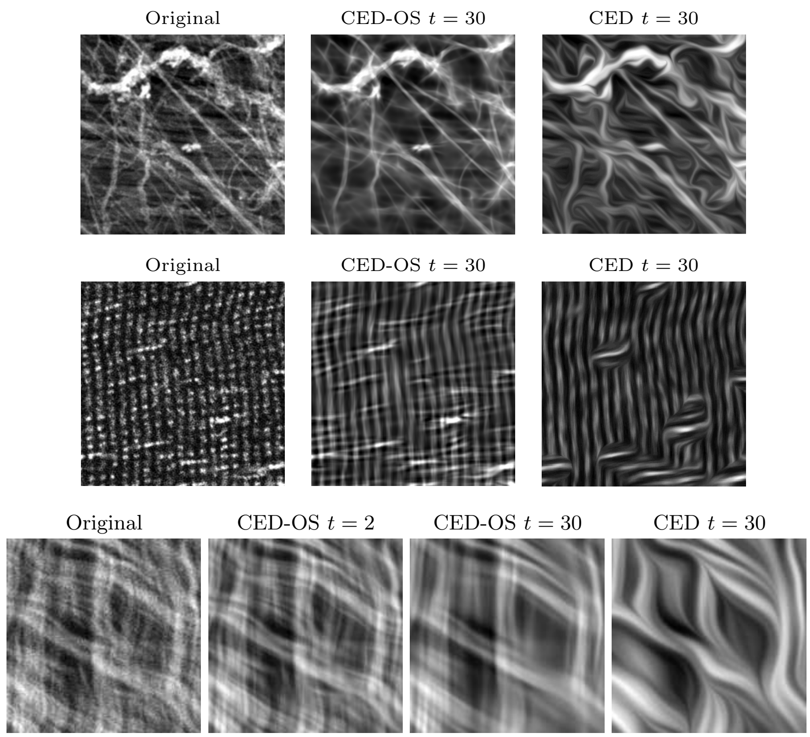

Fig. 7. Medical image applications. Top row: Result of coherence enhancing diffusion on orientations scores (CED-OS), see (4.1) and (4.4), and standard coherence enhancing diffusion (CED) directly on the image, see (2.5), of bone-tissue. Middle row: Result of (CED-OS) and (CED) of 2-photon microscopy images of a muscle cell. Bottom row : Result of (CED-OS) and(CED) on medical images of collageen fibers of the heart. All these applications clearly show that coherence enhancing diffusion on orientation scores (CEDOS) properly enhances crossing fibers whereas (CED) fails at crossings.

$|\kappa|^{-1}$ if κ is constant. Moreover, along horizontal curves we have (3.29), see Figure 8. Here we note that $\{\partial_\theta, \partial_\xi + \kappa\partial_\theta, \partial_\eta\}$ are (in contrast to $\frac{1}{\beta}\{\beta\partial_\theta, \partial_\xi, \partial_\eta\}$) not orthonormal with respect to the $(\cdot,\cdot)_\beta$ inner product (3.39). Therefore we are going to introduce the gauge-coordinates, aligned with the optimally fitting exponential curve

$$s \mapsto g\ \exp(s\sum_{i=1}^{3} c_*^i(g,t)A_i), \qquad \mathbf{c}_*(g,t) = (c_*^\theta(g,t), c_*^\xi(g,t), c_*^\eta(g,t)) \in \mathbb{R}^3,$$

with $\|\mathbf{c}_*\|_\beta = (c_*^\theta)^2 + \beta^2(c_*^\xi)^2 + \beta^2(c_*^\eta)^2 = 1$, to the orientation score data $|U(\cdot,t)|$ at position $g \in SE(2)$ at time $t > 0$. These gauge-directions are (for $c_*^\xi > 0$) given by

$$\begin{cases} \partial_a = \beta^2\sqrt{(c_*^\xi)^2 + (c_*^\eta)^2}\partial_\theta - \frac{c_*^\theta c_*^\xi}{\sqrt{(c_*^\xi)^2+(c_*^\eta)^2}}\partial_\xi - \frac{c_*^\theta c_*^\eta}{\sqrt{(c_*^\xi)^2+(c_*^\eta)^2}}\partial_\eta \\ \partial_b = \beta(c_*^\xi\partial_\xi + c_*^\eta\partial_\eta + c_*^\theta\partial_\theta) \\ \partial_c = \frac{-c_*^\eta}{\sqrt{(c_*^\xi)^2+(c_*^\eta)^2}}\partial_\xi + \frac{c_*^\xi}{\sqrt{(c_*^\xi)^2+(c_*^\eta)^2}}\partial_\eta\ . \end{cases}$$

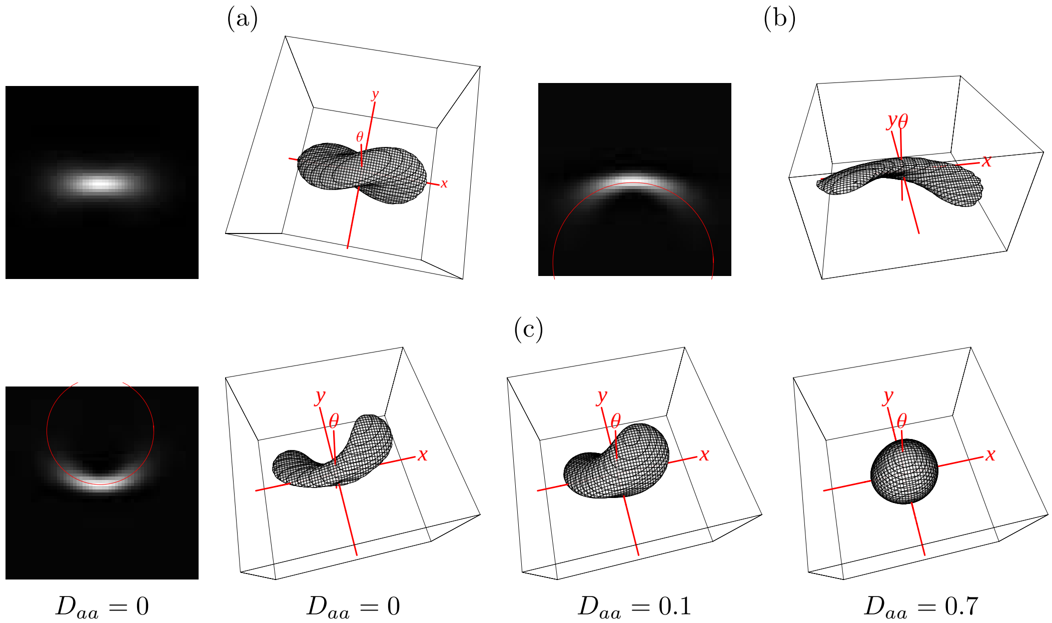

FIG. 8. Illustrations of heat-kernels $K_t^D : SE(2) \to \mathbb{R}^+$ on $SE(2)$ for different parameter values. (a): $D = \mathrm{diag}\{D_{11}, D_{22}, D_{22}\}$ in left-invariant coordinate frame $\{\partial_\theta, \partial_\xi, \partial_\eta\}$, Left: heat-kernel integrated over θ, $D_{11} = D_{33} = 0.003$, $\kappa = 0$, $D_{22} = 1$, and $\beta = 1$. (b): shows the effect of nonzero κ. Parameters $\kappa = -0.04$, $D_{aa} = D_{cc} = 0$, $D_{bb} = 1$, and $\beta = 1$, $d_H = 0$ with respect to frame $\{\partial_a, \partial_b, \partial_c\}$, see (4.3).(c): Shows the effect of varying $D_{aa} = D_{cc}$. Parameters $\kappa = 0.06$, $\beta = 0.1$ and $D_{bb} = 1$. As D_{aa} increases from 0 to 1, the resulting Green's function becomes more and more isotropic.

Note that the gauge-vector is along the best exponential curve-fit direction, i.e. $\partial_b = \beta \mathbf{c}_*$ and $\mathrm{span}\{\partial_a, \partial_c\} \equiv (\mathbf{c}_*)^\perp$. For geometric understanding it helps to consider the gauge-tangentvectors in ball-coordinates (d_H, α) with respect to the basis of left-invariant vector fields $\{\partial_\theta, \partial_\xi, \partial_\eta\}$ so that it becomes obvious which rotation in $SO(3)$ (or rather which class of rotations in $SO(3)/SO(2) \equiv S^2$, if we do not distinguish between directions in plane $(\mathbf{c}_*)^\perp$) is required to map the standard left-invariant basis $\{\partial_\theta, \partial_\xi, \partial_\eta\}$ into the basis gauge-coordinates, see Figure 9.

The gauge-directions in ball-coordinates read

$$\begin{cases} \partial_a = -\cos\alpha\, \cos d_H\, \partial_\xi - \cos\alpha\, \sin d_H\, \partial_\eta + \beta \sin\alpha\, \partial_\theta\ , \\ \partial_b = \sin\alpha\, \cos d_H\, \partial_\xi + \sin\alpha\, \sin d_H\, \partial_\eta + \beta\cos\alpha \partial_\theta\ , \\ \partial_c = -\sin d_H\, \partial_\xi + \cos d_H\, \partial_\eta\ , \end{cases} \tag{4.3}$$

where the Euler-angles read, where we recall (3.46),

$$\alpha = \arccos\left(\mathrm{sign}(c_*^\xi)\, c_*^\theta\right) = \arccos \frac{\kappa}{\sqrt{\kappa^2+\beta^2}}, \qquad d_H = \arg(c_*^\xi + i\, c_*^\eta).$$

Here the function d_H which maps U to $d_H(U)(g,t) = \arg(c_*^\xi(g,t) + i\, c_*^\eta(g,t))$ represents the "deviation from horizontality", as it tells us how much the tangent vector of the

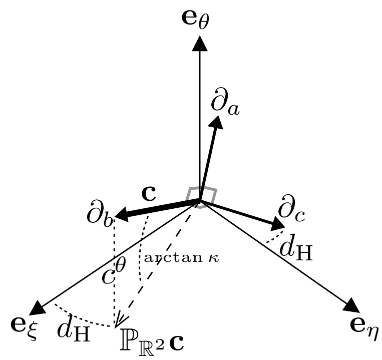

Fig. 9. Illustration of curvature κ and deviation from horizontality d_H and the gauge frame (4.3). For visualization reasons, the lengths of the vectors are arbitrary. The true lengths are given by $\|\mathbf{c}_*\|_\beta = \|\mathbf{e}_\theta\|_\beta = \|\mathbf{e}_\xi\|_\beta = \|\mathbf{e}_\eta\|_\beta = 1$ and $\|\partial_a\|_\beta = \|\partial_b\|_\beta = \|\partial_c\|_\beta = \beta$. Recall from part I of this article that $\mathbf{e}_\theta \leftrightarrow \partial_\theta$, $\mathbf{e}_\xi \leftrightarrow \partial_\xi$, $\mathbf{e}_\eta \leftrightarrow \partial_\eta$.

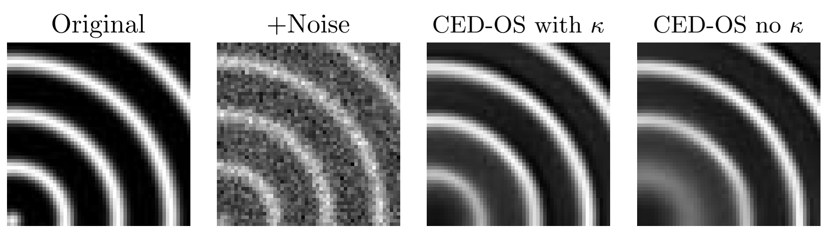

Fig. 10. Shows the effect of including curvature $\kappa = (\kappa_{est}(|U|))(g,t)$ on a noisy test image f in the final result of the CED-OS method, [22],[17], of $\Upsilon_\psi f = \mathcal{W}_\psi^* \Phi \mathcal{W}_\psi$, where ψ is the kernel illustrated in Fig.3(e,f) of part I of this article and where operator Φ is the non-linear diffusion (4.4) stopped at time $t = 30$. At $t = 30$ the effect is visible: the circle with highest curvature is blurred if no curvature is taken into account.

optimally fitting exponential curve (tangent spiral) points out of the horizontal plane, [22],[21], see Figure 11.

Remark 4.1. In some cases (for example if the image f has many identical parallel curves) it is sometimes better to use the *horizontal* curvature estimates (3.48) rather than the curvature estimates (3.46), [22]. In these cases one must set $d_H = 0$.

The diagonal diffusion generator along the left-invariant gauge vector fields is

$$D_{aa}(\partial_a)^2 + D_{bb}(\partial_b)^2 + D_{cc}(\partial_c)^2 = \begin{pmatrix} \beta\partial_\theta & \partial_\xi & \partial_\eta \end{pmatrix} M_{\alpha,d_H}^T \begin{pmatrix} D_{aa} & 0 & 0 \\ 0 & D_{bb} & 0 \\ 0 & 0 & D_{cc} \end{pmatrix} M_{\alpha,d_H} \begin{pmatrix} \beta\partial_\theta \\ \partial_\xi \\ \partial_\eta \end{pmatrix},$$

where $M_{\alpha,d_H} = \begin{pmatrix} \sin\alpha & -\cos\alpha\cos d_H & -\cos\alpha\sin d_H \\ \cos\alpha & \cos d_H \sin\alpha & \sin\alpha \sin d_H \\ 0 & -\sin d_H & \cos d_H \end{pmatrix}$ is the rotation matrix in $SO(3)$ that maps the left-invariant vector fields $\{\beta\partial_\theta, \partial_\xi, \partial_\eta\}$ onto the gauge-frame $\{\partial_a, \partial_b, \partial_c\}$. This

Original +Noise CED-OS with d_H CED-OS no d_H

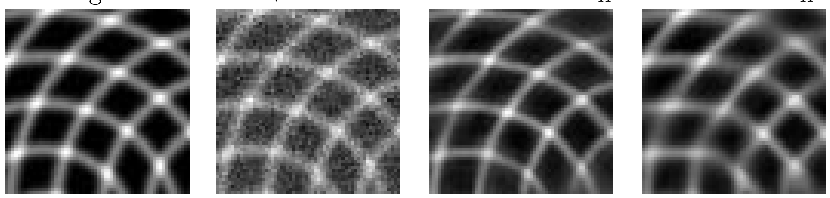

FIG. 11. Shows the effect of including "deviation from horizontality" $d_H(U)(g,t) = \arg(c_*^{\xi}(g,t) + i\, c_*^{\eta}(g,t)) \geq 0$ on a noisy test image f in the final result $\Upsilon_{\psi} f = \mathcal{W}_{\psi}^{*} \Phi \mathcal{W}_{\psi}$, where ψ is the kernel illustrated in Fig.3(e,f) of part I of this article and where the operator Φ is the nonlinear diffusion (4.4) stopped at time $t = 24$ using only 4 equidistant samples on the circle. At $t = 24$ the result without deviation from horizontality (using curvature estimation (3.48)) clearly shows that the lines bias towards the sampled angles 0,$\pi/4$, $\pi/2$ and $3\pi/4$. If we include deviation from horizontality (using curvature estimation (3.46)) this problem does not occur, and even with only for 4 samples on the torus we are able to handle these X-crossing correctly.

leads to the following nonlinear evolution equations on orientation scores

$$\begin{cases} \partial_t U(g,t) = (\ \beta\partial_\theta\ \partial_\xi\ \partial_\eta\ ) M_{\alpha,d_H}^{T} \begin{pmatrix} D_{aa} & 0 & 0 \\ 0 & D_{bb} & 0 \\ 0 & 0 & D_{cc} \end{pmatrix} M_{\alpha,d_H} \begin{pmatrix} \beta\partial_\theta \\ \partial_\xi \\ \partial_\eta \end{pmatrix} U(g,t),\ \ t>0, \\ U(g,t=0) = \mathcal{W}_\psi[f](g) \text{ for all } g \in SE(2), \end{cases} \tag{4.4}$$

where we again used short notation $D_{ii} = (D_{ii}(U))(g,t)$, for $i = a,b,c$. Now again we set $D_{bb} = 1$ and $(D_{aa}(U))(g,t) = (D_{cc}(U))(g,t) = e^{-\frac{(s(|U|)(g,t))^2}{c}}, c > 0$, where orientation confidence $s(|U|)(g,t)$, recall (4.2), is now expressed in Gauge-coordinates:

$$s(g,t) = \max\{-\Delta_{\mathbf{c}_*^{\perp}} |U(\cdot,t)|(g), 0\} = \max\{-\left((\partial_a)^2 |U(\cdot,t)| + (\partial_c)^2 |U(\cdot,t)|\right)(g), 0\}.$$

and the conductivity matrix in (4.4) equals

$$\frac{1}{\beta^2+\kappa^2} \begin{pmatrix} \kappa^2 + D_{aa}\beta^2 & \kappa\beta(1-D_{aa})\cos d_H & \kappa\beta(1-D_{aa})\sin d_H \\ \kappa\beta(1-D_{aa})\cos d_H & D_{aa}(\kappa^2+\beta^2) + (1-D_{aa})\beta^2\cos^2 d_H & \cos d_H \sin d_H \beta^2 (1-D_{aa}) \\ \kappa\beta(1-D_{aa})\sin d_H & \cos d_H \sin d_H \beta^2(1-D_{aa}) & \beta^2 + D_{aa}\kappa^2 + (D_{aa}-1)\beta^2\cos^2 d_H \end{pmatrix}.$$

See Figure 8 for an illustration of the special case D_{bb} is constant, $D_{aa} = D_{cc} = 0$, $d_H = 0$, which despite the strong degree of degeneracy still leads to a smooth and useful Green's function since the Hörmander condition, recall subsection 5.3 part I of this article, is satisfied. Furthermore, see Figure 10 and Figure 11 for illustrations of the practical relevance of respectively κ and d_H in the gauge-coordinate frame (4.3).

Appendix A. Derivation of the geodesics in P_Y by means of reduction of Pfaffian systems using Noether's Theorem . In this section we apply the Bryant-Griffith approach [6] on the Marsden-Weinstein reduction for Hamiltonian systems [30] admitting a Lie group of symmetries on Euler-Lagrange equations associated to the functional $\int \sqrt{\kappa^2(s)+\epsilon}\,\mathrm{d}s$, to explicitly derive the solution curves $s \mapsto \gamma(s)$ in $SE(2)$. In [17]Ch:7.1 we derived the curvature of the minimizer of $\int \sqrt{\kappa^2(s)+\epsilon}\,\mathrm{d}s$ by solving an ODE for κ that we derived from Euler-Lagrange minimization, similar to Mumford's approach to the elastica functional [31]. Here we derive the same equation, in a more abstract way, avoiding extensive computations, by means of symplectic geometry. Moreover we will derive an important underlying conservation law and by the Marsden-Weinstein reduction we derive the curves themselves (rather than just their curvatures [17]Ch:7.1)! The formulae that we shall derive (A.6) for the geodesics are much simpler than the formulae for the corresponding elastica curves as they do not involve special functions. For small $\beta > 0$ the geodesics are very close to the elastica curves and could be a nice practical alternative to the non-left-invariant (i.e. coordinate dependent) B-spline interpolations between two local orientations, [16], in vector graphics applications.

Although not discussed here, we stress that there is a fundamental relation between products of Green's functions discussed in (section 4 of) Part I of this article and these curves: The Brownian unconditional Brownian bridge measure of the contour-enhancement process concentrates on the geodesics as the expected lifetime, $E(T) = \frac{1}{\alpha} \to 0$, see [17]App. B.

Consider the manifold $Q = SE(2) \times \mathbb{R}^+ \times \mathbb{R} \times \mathbb{R}$ with coordinates $(x, y, e^{i\theta}, \sigma, \kappa, t)$, where $\sigma = \|\mathbf{x}'(t)\|$ so that $\mathrm{d}s = \sigma \mathrm{d}t$. On Q we consider the Pfaffian equations

$$\theta^1 := \mathrm{d}\mathcal{A}^2 - \sigma \mathrm{d}t = 0, \quad \theta^2 := \mathrm{d}\mathcal{A}^3 = 0, \quad \theta^3 := \mathrm{d}\theta - \kappa\sigma \mathrm{d}t = 0, \tag{A.1}$$

note that these Pfaffian equations uniquely determine the horizontal part $I(Q)$ of the dual tangent space $T^*(Q)$, where we recall that along horizontal curves we have $\frac{\mathrm{d}\theta}{\mathrm{d}s} = \sigma^{-1}\frac{\mathrm{d}\theta}{\mathrm{d}t} = \kappa$, $\langle \mathrm{d}\mathcal{A}^3, \mathbf{x}'(t)\rangle = 0$, $\langle \mathrm{d}\mathcal{A}^2, \mathbf{x}'(t)\rangle = \sigma$.

We would like to minimize the energy $\int \sqrt{\kappa^2 + \epsilon}\sigma dt$ under the side conditions (A.1), then the gradient of the energy should be linearly dependent on the gradient of the side condition and therefor we set

$$\psi = \sqrt{\kappa^2 + \epsilon}\sigma \mathrm{d}t + \lambda_1(\mathrm{d}\theta - \kappa\sigma\mathrm{d}t) + \lambda_2(\mathrm{d}\mathcal{A}^2 - \sigma\mathrm{d}t) + \lambda_3 \mathrm{d}\mathcal{A}^3$$

where λ_1, λ_2, λ_3 are Lagrange multipliers. Formally speaking, we consider the affine sub-bundle $Z = \{\, Z_q |\, q \in Q\} \equiv Q \times T(SE(2))^*$ of $T^*(Q)$ determined by

$$\begin{aligned} &Z_q = \{\, \sqrt{\kappa^2 + \epsilon}\sigma \mathrm{d}t\big|_q \in I_q \subset T_q^*(Q)\}, \\ &Z \equiv Q \times T(SE(2))^* \;\; \text{by the isomorphism} \;\; (q, \boldsymbol{\lambda}) \leftrightarrow \sqrt{\kappa^2 + \epsilon}\sigma\mathrm{d}t\big|_q + \sum_{k=1}^{3} \lambda_k \theta^k\big|_q \end{aligned}$$

Next we compute the exterior derivative of ψ :

$$\begin{aligned} \mathrm{d}\psi \;\; &= \sqrt{\kappa^2+\epsilon}\mathrm{d}\sigma \wedge \mathrm{d}t + \tfrac{\kappa\sigma}{\sqrt{\kappa^2+\epsilon}}\mathrm{d}\kappa \wedge \mathrm{d}t + \lambda_2 \mathrm{d}\theta \wedge \mathrm{d}\mathcal{A}^3 + \mathrm{d}\lambda_2 \wedge \mathrm{d}\mathcal{A}^2 - \mathrm{d}\lambda_2 \wedge \sigma\mathrm{d}t - \lambda_3\mathrm{d}\theta \wedge \mathrm{d}\mathcal{A}^2 \\ &\quad -\lambda_2\mathrm{d}\sigma \wedge \mathrm{d}t + \mathrm{d}\lambda_3 \wedge \mathrm{d}\mathcal{A}^3 + \mathrm{d}\lambda_1 \wedge \mathrm{d}\theta - \kappa\sigma\mathrm{d}\lambda_1 \wedge \mathrm{d}t - \sigma\lambda_1\mathrm{d}\kappa \wedge \mathrm{d}t - \kappa\lambda_1\mathrm{d}\sigma \wedge \mathrm{d}t \end{aligned}$$

where we used Cartan's structural equation (B.10): $\mathrm{d}\mathrm{d}\mathcal{A}^3 = -\mathrm{d}\theta \wedge \mathrm{d}\mathcal{A}^2$, $\mathrm{d}\mathrm{d}\mathcal{A}^2 = \mathrm{d}\theta \wedge \mathrm{d}\mathcal{A}^3$. The exterior derivative $\mathrm{d}\psi$ determines the characteristic curves (i.e. the geodesics) by

$$\gamma'(t) \rfloor \mathrm{d}\psi_{\gamma(t)} = 0, \qquad \text{and } \gamma^*\mathrm{d}t \neq 0.$$

So the Pfaffian equations for decent parameterizations satisfying $\gamma^*\mathrm{d}t \neq 0$ are given by

$$\begin{cases} \partial_{\lambda_1}\rfloor \mathrm{d}\psi = \mathrm{d}\theta - \kappa\sigma \mathrm{d}t = 0 \\ \partial_{\lambda_2}\rfloor \mathrm{d}\psi = \mathrm{d}\mathcal{A}^2 - \sigma \mathrm{d}t = 0 \\ \partial_{\lambda_3}\rfloor \mathrm{d}\psi = \mathrm{d}\mathcal{A}^3 = 0 \\ \partial_{\sigma}\rfloor \mathrm{d}\psi = (\sqrt{\kappa^2+\epsilon} - \lambda_1\kappa - \lambda_2)\mathrm{d}t = 0 \\ \partial_{\kappa}\rfloor \mathrm{d}\psi = \sigma(\kappa(\kappa^2+\epsilon)^{-1/2} - \lambda_1)\mathrm{d}t = 0 \\ -\partial_{\theta}\rfloor \mathrm{d}\psi = \mathrm{d}\lambda_1 - \lambda_2\mathrm{d}\mathcal{A}^3 + \lambda_3\mathrm{d}\mathcal{A}^2 = 0 \\ -\partial_{\xi}\rfloor \mathrm{d}\psi = \mathrm{d}\lambda_2 - \lambda_3\mathrm{d}\theta = 0 \\ -\partial_{\eta}\rfloor \mathrm{d}\psi = \mathrm{d}\lambda_3 + \lambda_2\mathrm{d}\theta = 0 \end{cases} . \tag{A.2}$$

The first three equations represent the horizontality restriction, the two equations in the middle represent the Euler-Lagrange optimization of the energy and the last three equations provide the Lagrange multipliers

$$\lambda_1 = \tfrac{\kappa}{\sqrt{\kappa^2+\epsilon}} = z\ , \quad \lambda_2 = \sqrt{\epsilon}\sqrt{1-z^2}\ , \quad \mathrm{d}z + \lambda_3\sigma\mathrm{d}t = \mathrm{d}z + \lambda_3\mathrm{d}s \Rightarrow \lambda_3 = -\dot{z}, \tag{A.3}$$

by employing Noether's theorem and an invariance group of symmetries of ψ (which is defined as a group acting on Q such that the induced action η on $T^*(Q)$ satisfies $\eta_g(Z) = Z$ for all $g \in G$) as will briefly explain next. In our case the action η on $T^*(Q)$ is induced by the left action of $SE(2)$ on itself) of the minimization problem.

Noether's theorem says that the momentum mapping $m : Z \to SE(2)^*$ given by

$$\langle m(p), \xi\rangle = (\xi\rfloor\psi)(p), \qquad p \in Z,$$

is constant along the characteristic curves.

Now the momentum mapping is invariant under the co-adjoint representation

$$m(\eta_g(p)) = (\mathrm{Ad}_{g^{-1}})^* m(p), \tag{A.4}$$

where $\eta_g(p = (g', \kappa, \sigma, \lambda)) = (g\, g', \kappa, \sigma, (\mathrm{Ad}_{g^{-1}})^*\lambda)$, so that $\eta_g^*\psi = \psi$ and $(\eta_g)\xi = (\mathrm{Ad}_g)\xi$, form which it indeed follows that

$$\begin{aligned} \langle m(\eta_g p), \xi\rangle &= (\xi\rfloor\psi)(\eta_g(p)) = ((\eta_g)_*\xi\rfloor(\eta_g)^*\psi)(p) \\ &= ((\mathrm{Ad}_g)\xi\rfloor(\eta_g)^*\psi)(p) = (\xi\rfloor(\mathrm{Ad}_{g^{-1}})_*\psi)(p) \\ &= \langle(\mathrm{Ad}_{g^{-1}})_* m(p), \xi\rangle \end{aligned}$$

for all $\xi \in T((SE(2))_t)$. It can be verified that the co-adjoint orbits of $SE(2)$ are given by $\lambda_2^2 + \lambda_3^2 = c^2\epsilon \geq 0,\ \ c > 0$. Consequently, the geodesics are contained in the co-adjoint orbits and we get the following *preservation law* that holds along the characteristic curves:

$$(\dot{z}(s))^2 + \epsilon - c^2\epsilon = \epsilon(z(s))^2, \qquad s > 0, \tag{A.5}$$

where the normalized curvature $z(s) = \frac{\kappa(s)}{\sqrt{\kappa^2(s)+\epsilon}}$ satisfies $|z| < 1$. Note that

$$\ddot{z} = \epsilon z \Leftrightarrow \dot{z}\ddot{z} = \epsilon\dot{z}z \Leftrightarrow (\dot{z}(s))^2 = \epsilon(z(s))^2 + C, C \in \mathbb{R}.$$

As observed by Bryant-Griffiths [6]p.543-544 (with slightly different conventions) the last three equations of (A.2) can be written

$$\mathrm{d}\hat{\lambda} = \hat{\lambda}g^{-1}\mathrm{d}g \Leftrightarrow \mathrm{d}(\hat{\lambda}\cdot g^{-1}) = \mathrm{d}\left(\widehat{(\mathrm{Ad}_{g^{-1}})^*}\cdot\lambda\right) = 0$$

where $\hat{\lambda}=(-\lambda_3,\lambda_2,\lambda_1)$ and where the matrix form of the Cartan connection equals,

$$g^{-1}\mathrm{d}g=\begin{pmatrix}\cos\theta & -\sin\theta & x\\ \sin\theta & \cos\theta & y\\ 0 & 0 & 1\end{pmatrix}^{-1}\mathrm{d}\begin{pmatrix}\cos\theta & -\sin\theta & x\\ \sin\theta & \cos\theta & y\\ 0 & 0 & 1\end{pmatrix}=\begin{pmatrix}0 & -\mathrm{d}\theta & \mathrm{d}\mathcal{A}^2\\ \mathrm{d}\theta & 0 & \mathrm{d}\mathcal{A}^3\\ 0 & 0 & 0\end{pmatrix}$$

where both Lie-algebra and Lie-group are embedded in the group of invertible 3×3 matrices. Consequently, by Noether's theorem we have $\hat{\lambda}=\hat{\mu}\cdot g$, for some constant $\hat{\mu}=(-\mu_3,\mu_2,\mu_1)$, or more explicitly we have

$$\left\{\begin{array}{l} z=\mu_1-\mu_3 x+\mu_2 y\\ \dot{z}=-\mu_3\cos\theta+\mu_2\sin\theta\\ \sqrt{\epsilon(1-z^2)}=\mu_3\sin\theta+\mu_2\cos\theta, \qquad \text{with } \mu_2^2+\mu_3^2=c^2\epsilon.\end{array}\right.$$

Next we choose $h_0=\begin{pmatrix}-\frac{\mu_3}{c\sqrt{\epsilon}} & -\frac{\mu_2}{c\sqrt{\epsilon}} & \frac{\mu_1\mu_3}{c^2\epsilon}\\ \frac{\mu_2}{c\sqrt{\epsilon}} & -\frac{\mu_3}{c\sqrt{\epsilon}} & -\frac{\mu_1\mu_2}{c^2\epsilon}\\ 0 & 0 & 1\end{pmatrix}^{-1}\in SE(2)$, so that $\hat{\mu}\cdot h_0^{-1}=(\sqrt{\epsilon}c,0,0)$ and use left-invariance $g=h_0^{-1}\tilde{g}$, $\tilde{g}\equiv(\tilde{x},\tilde{y},e^{i\tilde{\theta}})$ then we get $\hat{\lambda}=\hat{\mu}\cdot g=(c\sqrt{\epsilon},0,0)\cdot\tilde{g}$, i.e.

$$\tilde{x}=\tfrac{z}{c\sqrt{\epsilon}},\quad c\sqrt{\epsilon}\cos\tilde{\theta}=c\sqrt{\epsilon}\dot{\tilde{x}}=\dot{z},\ \text{and}\ -\sqrt{\epsilon(1-z^2)}=-\sqrt{\epsilon}c\sin\tilde{\theta}=c\sqrt{\epsilon}\dot{\tilde{y}}$$

and consequently we have

$$\tilde{x}(s)=(\sqrt{\epsilon}c)^{-1}z(s),\quad \tilde{y}(s)=\tilde{y}(0)+\tfrac{1}{c}\int_0^s\sqrt{1-(z^2(\tau))}\,\mathrm{d}\tau,\quad \tilde{\theta}(s)=\tilde{\theta}(0)+\int_0^s\kappa(\tau)\,\mathrm{d}\tau.$$

So by solving (A.5) we have $z(s)=z_0\cosh(\sqrt{\epsilon}\,s)+\frac{z_0'}{\sqrt{\epsilon}}\sinh(\sqrt{\epsilon}\,s)$ and we get the surprisingly simple solution $g(s)=(x(s),y(s),\theta(s))=h_0^{-1}(\tilde{x}(s),\tilde{y}(s),\tilde{\theta}(s))$, i.e.

$$\left\{\begin{array}{l} x(s)=\frac{\mu_1\mu_3}{c^2\epsilon}-\frac{\mu_3}{c\sqrt{\epsilon}}\tilde{x}(s)-\frac{\mu_2}{c\sqrt{\epsilon}}\tilde{y}(s)\\ y(s)=\frac{-\mu_1\mu_2}{c^2\epsilon}+\frac{\mu_2}{c\sqrt{\epsilon}}\tilde{x}(s)-\frac{\mu_3}{c\sqrt{\epsilon}}\tilde{y}(s)\\ \theta(s)=\tilde{\theta}(s)+\arccos\left(-\frac{\mu_3}{c\sqrt{\epsilon}}\right)\end{array}\right. \text{with} \left\{\begin{array}{l} \tilde{x}(s)=\frac{z_0}{\sqrt{\epsilon}c}\cosh(\sqrt{\epsilon}s)+\frac{z_0'}{c\epsilon}\sinh(\sqrt{\epsilon}s)\\ \tilde{y}(s)=\tilde{y}_0+\frac{1}{c}\int_0^s\sqrt{1-c^2(\tilde{x}(\tau))^2\epsilon}\,\mathrm{d}\tau\\ \tilde{\theta}(s)=\arccos\left(\frac{z_0}{c}\sinh(\sqrt{\epsilon}\,s)+\frac{z_0'}{c\sqrt{\epsilon}}\cosh(\sqrt{\epsilon}s)\right)\end{array}\right., \tag{A.6}$$

where $c=\sqrt{1+\frac{(z_0')^2}{\epsilon}-z_0^2}$. Now we have 6 unknown parameters $\mu_1,\mu_3,z_0,z_0',\tilde{y}(0),L$, to ensure the given boundary conditions

$$\left\{\begin{array}{l} g(0)=(x(0),y(0),e^{i\theta(0)})=g_0:=(x_0,y_0,e^{i\theta_0}),\\ g(L)=(x(L),y(L),e^{i\theta(L)})=g_1=(x_1,y_1,e^{i\theta_1})\end{array}\right.$$

By means of left-invariance we can always ensure (by multiplying from the left with g_1^{-1}) that $g_1=e$, so $\theta_1=0,x_1=0,y_1=0$. In this case straightforward computations yield

$$\begin{array}{l} \mu_1=z_0+\mu_3x_0-\mu_2y_0,\\ \mu_2=c\sqrt{\epsilon}\sin(\arccos\left(\frac{-\mu_3}{c\sqrt{\epsilon}}\right)),\\ \mu_3=-z_0'\cos\theta_0+\sqrt{\epsilon}\sin\theta_0\sqrt{1-z_0^2},\\ c=\sqrt{\frac{\mu_2^2+\mu_3^2}{\epsilon}}=\sqrt{1+\frac{(z_0')^2}{\epsilon}-(z_0)^2}\\ \tilde{y}(0)=\frac{-\mu_3y_0-\mu_2x_0}{c\sqrt{\epsilon}},\end{array}\qquad L=\left\{\begin{array}{l} \frac{-1}{\sqrt{\epsilon}}\log\left(\frac{\mu_3}{\sqrt{\epsilon}z_0}\right)\text{ if } c=1\\ \\ \frac{1}{\sqrt{\epsilon}}\log\left(\frac{-\mu_3+\sqrt{-(z_0')^2+(z_0)^2\epsilon+\mu_3^2}}{z_0'+z_0\sqrt{\epsilon}}\right)\\ \text{if } c>1,\mu_3<0,z_0'+z_0\sqrt{\epsilon}>0\\ \frac{1}{\sqrt{\epsilon}}\log\left(\frac{-\mu_3-\sqrt{-(z_0')^2+(z_0)^2\epsilon+\mu_3^2}}{z_0'+z_0\sqrt{\epsilon}}\right)\\ \text{if } c<1,\mu_3<0,z_0'+z_0\sqrt{\epsilon}<0\end{array}\right.,\tag{A.7}$$

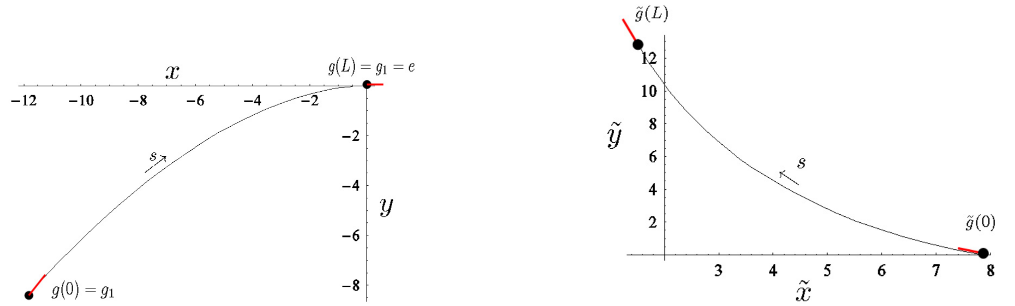

FIG. 12. Left figure: Illustration of a geodesic $s \mapsto g(s)$ computed by (A.6) and its affine relative $s \mapsto \tilde{g}(s) = h_0^{-1} g(s)$. Parameter settings $x_0 = -11.868$, $y_0 = -8.44337$, $\theta_0 = 51.95°$, $x_1 = y_1 = \theta_1 = 0$, $L = 15$, $\epsilon = 0.0125$, $z_0 = -0.1641$, $z_0' = 0.0183$, $c = 1$.

So all parameters are now expressed in the two unknown z_0 and z_0' which are determined by the two remaining boundary conditions:

$$\begin{cases} \frac{\mu_1\mu_3}{c^2\epsilon} - \frac{\mu_3}{c\sqrt{\epsilon}}\tilde{x}(L) - \frac{\mu_2}{c\sqrt{\epsilon}}\tilde{y}(L) = x_1, \\ -\frac{\mu_1\mu_2}{c^2\epsilon} + \frac{\mu_2}{c\sqrt{\epsilon}}\tilde{x}(L) - \frac{\mu_3}{c\sqrt{\epsilon}}\tilde{y}(L) = y_1. \end{cases} \tag{A.8}$$

Now since $SE(2)$ is a symmetric space [26] all points can be connected by a geodesic and we may expect that there indeed exist z_0 and z_0' such that (A.8) holds. Consequently, the singularities (which cause extreme problems in our numerical shooting algorithm [17]Ch:7.1) where $z(s_{max}) = 1$ occur always at $s_{max} \geq L$ (and if $\mu_3 \neq c\sqrt{\epsilon}$ then $s_{max} > L$). Next we explicitly verify that $s_{max} \geq L$ in 2 cases.

In case $c > 1, \mu_3 < 0$ and $z_0' + \sqrt{\epsilon} z_0 > 0$ we have

$$e^{\sqrt{\epsilon}L} = \frac{-\mu_3 + \sqrt{-(z_0')^2 + (z_0)^2\epsilon + \mu_3^2}}{z_0' + z_0\sqrt{\epsilon}}, \quad \text{and } e^{\sqrt{\epsilon}s_{max}} = \frac{-\sqrt{\epsilon} + \sqrt{(z_0')^2 - (z_0)^2\epsilon + \epsilon}}{z_0' + z_0\sqrt{\epsilon}} = \frac{\sqrt{\epsilon}(1+c)}{z_0' + z_0\sqrt{\epsilon}}$$

and indeed $-\mu_3 + \sqrt{-(z_0')^2 + (z_0)^2\epsilon + \mu_3^2} < 2\sqrt{\epsilon} < (1+c)\sqrt{\epsilon}$ so $L < s_{max}$.

In case $c < 1, \mu_3 > 0$ and $z_0' + \sqrt{\epsilon} z_0 < 0$ we have

$$e^{\sqrt{\epsilon}L} = \frac{-\mu_3 - \sqrt{-(z_0')^2 + (z_0)^2\epsilon + \mu_3^2}}{z_0' + z_0\sqrt{\epsilon}} \quad \text{and } e^{\sqrt{\epsilon}s_{max}} = \frac{-\sqrt{\epsilon} + \sqrt{(z_0')^2 - (z_0)^2\epsilon + \epsilon}}{z_0' + z_0\sqrt{\epsilon}} = \frac{\sqrt{\epsilon}(1+c)}{|z_0' + z_0\sqrt{\epsilon}|} = \frac{\sqrt{\epsilon}(1+c)}{-(z_0' + z_0\sqrt{\epsilon})}$$

and indeed we have $e^{\sqrt{\epsilon}s_{max}} \geq e^{\sqrt{\epsilon}L}$, since $\mu_3 + \sqrt{-(z_0')^2 + (z_0)^2\epsilon + \mu_3^2} \leq c\sqrt{\epsilon} + \sqrt{\epsilon(1-c^2) + c^2\epsilon} = \sqrt{\epsilon}(1+c)$. Equality is obtained if $\mu_3 = c\sqrt{\epsilon}$. See Figure 12.

Appendix B. Proof of Theorem 3.8 . Again we set $\{A_1, A_2, A_3\} = \{\partial_x, \partial_y, \partial_\theta\}$ as a basis for the Lie-algebra $T_e(SE(2))$ and $\{\mathcal{A}_1, \mathcal{A}_2, \mathcal{A}_3\} = \{\mathrm{d}\mathcal{R}(A_1), \mathrm{d}\mathcal{R}(A_2), \mathrm{d}\mathcal{R}(A_3)\} = \{\partial_\theta, \partial_\xi, \partial_\eta\}$ as a basis for the space $\mathcal{L}(SE(2))$ of left-invariant vector fields with corresponding dual basis $\{\mathrm{d}\mathcal{A}^1, \mathrm{d}\mathcal{A}^2, \mathrm{d}\mathcal{A}^3\} \subset (\mathcal{L}(SE(2)))^*$ as given in Theorem 3.1.

The Maurer-Cartan form $\omega : (SE(2), T(SE(2))) \to T_e(SE(2))$ is defined given by

$$\omega_g(Y_g) = (L_{g^{-1}})_* Y_g, \tag{B.1}$$

where $(L_{g^{-1}})_*$ denotes the push forward of the inverse left multiplication $h \mapsto L_g h = g^{-1}h$, i.e. $\omega_g(Y_g)\phi = Y_g(\phi \circ L_{g^{-1}})$ for all $\phi : \Omega_e \to \mathbb{R}$ smooth defined on some local open set Ω_e around the unity e. Now recall from Theorem 3.1, that the left-invariant vector fields are obtained by the derivative $\mathrm{d}\mathcal{R}$ of the right-regular representation $g \mapsto \mathcal{R}_g\phi(h) = \phi(hg)$, i.e. $\mathcal{A}_i = \mathrm{d}\mathcal{R}(A_i)$. Now the Maurer-Cartan form does the reverse it "connects" each tangent spaces $T_g(SE(2))$ to $T_e(SE(2))$. To this end we note that

$$\lim_{h\downarrow 0} \frac{\phi(g\exp(hA_i)) - \phi(g)}{h} =: (\mathrm{d}\mathcal{R}(A_i))_g\phi = (\mathcal{A}_i)_g\phi = (L_g)_*A_i\phi = A_i(\phi \circ L_g) \in \mathbb{R} \quad \text{(B.2)}$$

for all $g \in SE(2)$ and all smooth $\phi : \Omega_g \to \mathbb{R}$. Therefore we have

$$(L_g)_*(L_{g^{-1}})_* = (L_{gg^{-1}})_* = I \Leftrightarrow \forall_{i\in\{1,2,3\}} \ : \ \omega \circ \mathrm{d}\mathcal{R}(A_i) = \omega(\mathcal{A}_i) = A_i \Leftrightarrow \omega \circ \mathrm{d}\mathcal{R} = I.$$

So by linearity and $\langle \mathrm{d}\mathcal{A}^i, \mathcal{A}_j\rangle = \delta_{ij}$ it is now clear that the coordinate dependent definition of the Cartan-Maurer form (B.1) indeed yields (3.15) in explicit coordinates.

Now we show that the Maurer-Cartan form indeed forms a Cartan-Ehresmann connection form, recall Definition 3.6, on the principal fiber bundle, recall Definition 3.5, $P = (SE(2), e, SE(2), \mathcal{L}(SE(2)))$. The first requirement in Definition 3.6 has been shown above, so let us verify the second requirement. Indeed a brief computation yields

$$\omega_{gh}((R_h)_*Y_g) = (L_{h^{-1}} \circ L_{g^{-1}})_*((R_h)_*Y_g) = (L_{h^{-1}})_* \circ (L_{g^{-1}})_* \circ (R_h)_*Y_g = \mathrm{Ad}(h^{-1})\omega_g Y_g\ . \quad \text{(B.3)}$$

Then we must show that equality (3.16) holds. This equality follows from the fact that left-multiplication L_g and right-multiplication R_g commute, since this implies that

$$(R_{g^{-1}}L_g)_* = (L_gR_{g^{-1}})_* = (L_g)_*(R_{g^{-1}})_* = (L_g)_*(R_{g^{-1}}L_g)_*(L_{g^{-1}})_*\ .$$

from which we indeed deduce that $\widetilde{\mathrm{Ad}}(g) = \mathrm{d}\mathcal{R} \circ \mathrm{Ad}(g) \circ \omega$. The adjoint representation $\mathrm{Ad} : SE(2) \to GL(T_e(SE(2)))$ coincides with the derivative of the conjugation automorphism $h \mapsto \mathrm{conj}(g)(h) = ghg^{-1}$ evaluated at e, i.e. $\mathrm{Ad}(g) = D_e\mathrm{conj}(g) = (R_{g^{-1}}L_g)_*$.

REMARK B.1. *Here $GL(T_e(SE(2)))$ stands for all linear operators on the Lie-algebra $T_e(SE(2))$. Note that each linear operator $\overline{Q} \in GL(T_e(SE(2))$ on $T_e(SE(2))$ is 1-to-1 related to a bilinear form Q on $(T_e(SE(2)))^* \times T_e(SE(2))$ by means of*

$$\langle B, \overline{Q}A\rangle = Q(B,A), \text{ for all } B \in (T_e(SE(2)))^*, A \in T_e(SE(2)) \text{ and}$$
$$\overline{Q} = \sum_{i=1}^{3} Q(\mathrm{d}\mathcal{A}^i, \cdot)\mathcal{A}_i.$$

So a basis for $GL(T_e(SE(2)))$ is given by $\{\overline{\mathrm{d}A^i \otimes A_j} \mid i,j = 1,2,3\}$. In this article, we omit the overline and again write $\mathrm{d}A^i \otimes A_j$ as it is clear from the context if we mean the bilinear form or the linear mapping.

Recall Definition 3.7 of an associated vector bundle and set

$$P = SE(2),\ M = e,\ G = SE(2),\ F = \mathcal{L}(SE(2)),\ \rho = \widetilde{\mathrm{Ad}}, \pi(g) = e,\ R_g u = u\, g, \quad \text{(B.4)}$$

where $\mathcal{L}(SE(2))$ denotes the Lie-algebra of left-invariant vector fields on $SE(2)$ and $\widetilde{\mathrm{Ad}}$ the adjoint representation of $SE(2)$ into $GL(\mathcal{L}(SE(2)))$ given by

$$\widetilde{\mathrm{Ad}}(g)X = (R_{g^{-1}}L_g)_*X, \qquad X \in \mathcal{L}(SE(2)), g \in SE(2). \quad \text{(B.5)}$$

A connection ω on a principal fiber bundle P is 1-to-1 related to a connection $\tilde{\omega}$ on the vector bundle $P \times_\rho F$ by means of

$$\omega = \sum_j A_j \otimes \mathrm{dx}^{\mathrm{j}} \leftrightarrow \tilde{\omega} = \sum_j \rho_*(A_j) \otimes \mathrm{dx}^{\mathrm{j}}, \quad \text{(B.6)}$$

where $\{\mathrm{d}x^j\}$ are dual forms on F, for details on this common bijection see [34]. In our case we have $F = \mathcal{L}(SE(2))$ and dual forms $\{\mathrm{d}\mathcal{A}^j\}_{j=1,2,3}$. Note that we applied the convention in Remark B.1. So in our case (B.4) the push-forward ρ_* of $\rho = \widetilde{\mathrm{Ad}}$ equals

$$\begin{aligned}(\widetilde{\mathrm{Ad}})_*(A_j) &= (\mathrm{d}\mathcal{R} \circ \mathrm{Ad}_*)\,(A_j) = (\mathrm{d}\mathcal{R} \circ \mathrm{ad} \circ \omega)(\mathcal{A}_j) \\ &= \widetilde{\mathrm{ad}}(\mathcal{A}_j) = [\,\cdot\,, \mathcal{A}_j]_{\mathcal{L}(SE(2))} = \sum_{i,k=1}^{3} c^k_{ij} \mathcal{A}_k \otimes \mathrm{d}\mathcal{A}^i.\end{aligned}$$

Thereby the connection-form on the vector bundle $SE(2) \times_{\widetilde{\mathrm{Ad}}} \mathcal{L}(SE(2))$ is given by

$$\tilde{\omega} = \sum_{j=1}^{3} \widetilde{\mathrm{ad}}(\mathcal{A}_j) \otimes \mathrm{d}\mathcal{A}^j = \sum_{i,j,k=1}^{3} c^k_{ij}\; \mathcal{A}_k \otimes \mathrm{d}\mathcal{A}^i \otimes \mathrm{d}\mathcal{A}^j, \tag{B.7}$$

where c^k_{ij} are the structure constants of the Lie group $SE(2)$, so $\widetilde{\mathrm{ad}}(\mathcal{A}_j)(\mathcal{A}_i) = [\mathcal{A}_i, \mathcal{A}_j] = \sum_{i,j,k=1}^{3} c^k_{ij} \mathcal{A}_k$. Now the non-zero structure constants are $-c^2_{13} = c^2_{31} = c^3_{12} = -c^3_{21} = 1$ and thereby (B.7) yields (3.17), where we also used $\mathrm{d}a \wedge \mathrm{d}b = \mathrm{d}a \otimes \mathrm{d}b - \mathrm{d}a \otimes \mathrm{d}b$.

Now from $\tilde{\omega}$ given by (B.7) one can construct the 9-connection 1-forms $\{\tilde{\omega}^k_j(\,\cdot\,)\}^3_{k,j=1}$ by (3.18) which together form a 3×3-matrix valued 1-form on the frame-bundle [36, p.353, p.359], where the sections are moving frames [36, p.354].

Let $\{\mu_k\}^3_{k=1}$ denote the sections in $(SE(2), T(SE(2)))$ which coincide respectively with the left-invariant vector fields $\{\mathcal{A}_k\}^3_{k=1}$. Then the Cartan connection D on (the vector bundle $SE(2) \times_{\widetilde{\mathrm{Ad}}} \mathcal{L}(SE(2))$ isomorphic to) tangent-bundle $(SE(2), T(SE(2)))$ equals

$$D := \mathrm{d} + \overline{\omega} \text{ with } \overline{\omega}(\mu_k)(\,\cdot\,) := \sum_{j=1}^{3} \tilde{\omega}^j_k(\,\cdot\,)\; \mu_j, \tag{B.8}$$

or more precisely, the covariant derivatives are given by,

$$\begin{aligned} D_{X|_{\gamma(t)}}(\mu(\gamma(t))) &:= (D\mu(\gamma(t)))(X|_{\gamma(t)}) \\ &= \sum_{k=1}^{3} \dot{a}^k(t)\, \mu_k(\gamma(t)) + \sum_{k=1}^{3} a^k(\gamma(t)) \sum_{j=1}^{3} \tilde{\omega}^j_k(X|_{\gamma(t)})\; \mu_j(\gamma(t)) \\ &= \sum_{k=1}^{3} \dot{a}^k(t)\, \mu_k(\gamma(t)) + \sum_{i,j,k=1}^{3} \dot{\gamma}^i(t)\, a^k(\gamma(t))\; \Gamma^j_{ik}\; \mu_j(\gamma(t)) \end{aligned} \tag{B.9}$$

with $\dot{a}^k(t) = \dot{\gamma}^i(t)(\mathcal{A}_i|_{\gamma(t)}\, a^k)(\gamma(t))$, for all curves $\gamma : \mathbb{R} \to SE(2)$ and tangent vectors $X|_{\gamma(t)} = \sum_{i=1}^{3} \dot{\gamma}^i(t)\;\; \mathcal{A}_i|_{\gamma(t)} \in T_{\gamma(t)}(SE(2))$ and all sections $\mu(\gamma(t)) = \sum_{k=1}^{3} a^k(\gamma(t))\; \mu_k(\gamma(t))$ and where the Christoffel symbols Γ^k_{ij}, [26, p.108], are constant $\Gamma^k_{ij} = \tilde{\omega}^k_j(\mathcal{A}_i) = -\tilde{\omega}(\mathrm{d}\mathcal{A}^k, \mathcal{A}_i, \mathcal{A}_j) = -c^k_{ij} = c^k_{ji}$. Now finally, the curvature 2-forms Ω^i_j for the moving frame $\{\mathcal{A}_1, \mathcal{A}_2, \mathcal{A}_3\}$ are $\Omega^i_j = \mathrm{d}\tilde{\omega}^i_j + \sum_{k=1}^{3} \tilde{\omega}^i_k \wedge \tilde{\omega}^k_j$, [36, p.317]. These curvature 2-forms are bijectively related, [36, p.322] to the Riemann-curvature tensor on the tangent bundle $(SE(2), T(SE(2)))$:

$$R^i_{jkl} = \Omega^i_j(\mathcal{A}_k, \mathcal{A}_l) \text{ and } \Omega^i_j = \frac{1}{2} \sum_{k,l=1}^{3} R^i_{jkl}\; \mathrm{d}\mathcal{A}^k \wedge \mathrm{d}\mathcal{A}^l\ .$$

Now by means of Maurer-Cartan's structural formula, [1], recall (3.31),

$$\mathrm{d}(\mathrm{d}\mathcal{A}^k) = -\frac{1}{2} \sum_{i,j,k=1}^{3} c^k_{ij} \mathrm{d}\mathcal{A}^{\mathrm{i}} \wedge \mathrm{d}\mathcal{A}^j, \tag{B.10}$$

we find by straightforward computation (using Einstein's summation convention)

$$
\begin{aligned}
\Omega^i_j &= c^i_{j\lambda}\mathrm{d}(\mathrm{d}\mathcal{A}^\lambda) + \mathrm{c}^{\mathrm{i}}_{\lambda\mathrm{k}}\mathrm{c}^{\lambda}_{\mathrm{jl}}\, \mathrm{d}\mathcal{A}^{\mathrm{k}} \wedge \mathrm{d}\mathcal{A}^{\mathrm{l}} = \tfrac{1}{2}\left(\mathrm{c}^{\mathrm{i}}_{\mathrm{k}\lambda}\mathrm{c}^{\lambda}_{\mathrm{lj}} + (\mathrm{c}^{\mathrm{i}}_{\mathrm{j}\lambda}\mathrm{c}^{\lambda}_{\mathrm{kl}} - \mathrm{c}^{\mathrm{i}}_{\mathrm{k}\lambda}\mathrm{c}^{\lambda}_{\mathrm{jl}})\right)\, \mathrm{d}\mathcal{A}^{\mathrm{k}} \wedge \mathrm{d}\mathcal{A}^{\mathrm{l}} \\
&= \tfrac{1}{2}(c^i_{k\lambda}c^\lambda_{lj} - c^i_{l\lambda}c^\lambda_{kj})\, \mathrm{d}\mathcal{A}^k \wedge \mathrm{d}\mathcal{A}^l = \tfrac{1}{2}c^i_{\lambda j}c^\lambda_{kl}\, \mathrm{d}\mathcal{A}^k \wedge \mathrm{d}\mathcal{A}^l = \tfrac{1}{2}R^j_{i,kl}\mathrm{d}\mathcal{A}^k \wedge \mathrm{d}\mathcal{A}^l,
\end{aligned}
\tag{B.11}
$$

where we used the Jacobi-identity $[X,[Y,Z]]+[Y,[Z,X]]+[Z,[X,Y]]=0$ in the third and fourth equality. For example for $Y=\mathcal{A}_l$, $Z=\mathcal{A}_j$, $X=\mathcal{A}_k$ we find $c^i_{k\lambda}c^\lambda_{lj}+c^i_{l\lambda}c^\lambda_{jk}+c^i_{j\lambda}c^\lambda_{kl}$. Now from (B.11) we deduce $R^i_{j,kl}=\frac{1}{2}c^i_{\lambda j}c^\lambda_{kl}$ from which the final result (3.20) follows.

Acknowledgements. The authors gratefully acknowledge Prof. David Mumford from Brown University, Providence, USA, for his good suggestions on the organization and formulation of this article. Moreover, the authors gratefully thank him for his thorough comments on the contents of earlier drafts of this article.

References

[1] M. A. Akivis and B.A. Rosenfeld. *Élie Cartan (1869-1951)*, volume 123. American Mathematical Society, Providence, 1993. Translations of Mathematical Monographs.

[2] N. Aronszajn. Theory of reproducing kernels *Trans. A.M.S.*, vol. 68, p.337–404, 1950.

[3] V.Arsigny, X. Pennec and N. Ayache. Bi-invariant Means in Lie Groups. Application to Left-invariant Polyaffine Transformations. Technical report, nr. 5885, INRIA, France, April 2006.

[4] V.Arsigny, P.Fillard, X. Pennec and N. Ayache. Geometric Means in a Novel Vector Space Structure on Symmetric Positive-Definite Matrices. SIAM Journal on Matrix Analysis and Applications, 29(1):328-347, 2006.

[5] J. August and S.W. Zucker. The curve indicator random field and markov processes. *IEEE-PAMI, Pattern Recognition and Machine Intelligence*, 25, 2003. Number 4.

[6] R. Bryant and P. Griffiths. Reduction for constrained variational problems and $(1/2)\int \kappa^2 \mathrm{d}s$. *American Journal of Mathematics*, 108(3):525–570, June 1986.

[7] R. Bryant and P. Griffiths and D. Grossman Exterior Differential Systems and Euler-Lagrange Partial Differential Equations . *Chicago Lectures in Mathematics*, 2003.

[8] G.S. Chirikjian and A.B. Kyatkin *Engineering applications of non-commutative harmonic analysis with emphasis on rotation and motion groups.* CRC Press LLC, USA, 2001.

[9] G. Citti and A. Sarti A cortical based model of perceptional completion in the roto-translation space. *Journal of Mathematical Imaging and Vision*, 24 (3):307-326, 2006.

[10] G.-H. Cottet and L.Germain Image processing through reaction combined with non-linear diffusion. *Mathematics of Computation, 61:659–667, 1993.*

[11] M. Duits and R. Duits. Unitary wavelet transforms based on reducible representations of the affine group. In preparation.

[12] R. Duits. *Perceptual Organization in Image Analysis.* PhD thesis, Eindhoven University of Technology, Department of Biomedical Engineering, The Netherlands, 2005. A digital version is available on the web URL: http:// www.bmi2.bmt.tue.nl/Image-Analysis/People/RDuits/THESISRDUITS.pdf.

[13] R. Duits, M. Felsberg, G. Granlund, and B.M. ter Haar Romeny. Image analysis and reconstruction using a wavelet transform constructed from a reducible representation of the euclidean motion group. *International Journal of Computer Vision*. Volume 72, issue 1, p.79-102, April 2007.

[14] R. Duits, M. Duits, M. van Almsick and B.M. ter Haar Romeny. Invertible Orientation Scores as an Application of Generalized Wavelet Theory. *Image Processing, Analysis, Recognition, and Understanding*. Volume 17, Nr. 1: p. 42–75 , 2007.

[15] R. Duits, M. van Almsick, M. Duits, E. Franken, and L.M.J. Florack. Image processing via shift-twist invariant operations on orientation bundle functions. In Niemann Zhuralev et al. Geppener, Gurevich, editor, *7th International Conference on Pattern Recognition and Image Analysis: New Information Technologies*, pages 193–196, St.Petersburg, October 2004.

[16] R. Duits and M. van Almsick. The Explicit Solutions of Linear Left-Invariant Second Order Stochastic Evolution Equations on the 2D-Euclidean Motion Group *Quarterly of Applied Mathematics* American Mathetical Society, Volume 66, nr. 1, p.27–67, April 2008.

[17] R.Duits and E.M. Franken Left-invariant Stochastic Evolution Equations on $SE(2)$ and its Applications to Contour Enhancement and Contour Completion via Invertible Orientation Scores. *arXiv:*

0711.0951v4 , see *http://arxiv.org/abs/0711.0951* Also available as CASA report nr.35, 2007, Eindhoven University of Technology, *http://www.win.tue.nl/casa/research/casareports/2007.html*

[18] R.Duits and E.M. Franken Left-invariant Parabolic Evolutions on $SE(2)$ and Contour Enhancement via Invertible Orientation Scores, *Part I: Linear Left-invariant Diffusion Equations on SE(2).* Submitted to Quarterly of Applied Mathematics 2008.

[19] N. Dungey, A. F. M. ter Elst, and D. W. Robinson. *Analysis on Lie groups with polynomial growth*, volume 214. Birkhauser-Progress in Mathematics, Boston, 2003.

[20] E.Franken, R.Duits and B.M. ter Haar Romeny", Nonlinear Diffusion on the Euclidean Motion Group. *Proc. of the first international conference on Scale Space and Variational Methods in Computer Vision*, 461–472, 2007.

[21] E.M. Franken and R. Duits and B.M. ter Haar Romeny Curvature estimation for Enhancement of Crossing Curves. *Mathematical Methods for Biomedical Image Analysis (MMBIA), IEEE workshop ICCV (receiving the best paper award), Rio de Janeiro, 2007.*

[22] E.M. Franken and R. Duits Crossing-Preserving Coherence-Enhancing Diffusion on Invertible Orientation Scores. *Accepted, to appear in International Journal of Computer Vision, 2008.*

[23] B. Gaveau. Principe de moindre action, propagation de la chaleur et estimees sous elliptiques sur certains groupes nilpotents. *Acta mathematica*, 139:96–153, 1977.

[24] W. Hebisch. Estimates on the semigroups generated by left-invariant operators on lie groups. *Journal fuer die reine und angewandte Mathematik*, 423:1–45, 1992.

[25] L. Hormander. Hypoellptic second order differential equations. *Acta Mathematica*, 119:147–171, 1968.

[26] J. Jost. *Riemannian Geometry and Geometric Analysis* Springer Heidelberg-New York, ed. 4, 2005.

[27] S. N. Kalitzin, B. M. ter Haar Romeny, and M. A. Viergever. Invertible apertured orientation filters in image analysis. *Int. Journal of Computer Vision*, 31(2/3):145–158, April 1999.

[28] S. Kobayashi and K. Nomizu Foundation of Differential Geometry, Vol.1. Wiley Classics Library, New York, 1963.

[29] G.W. Mackey, Imprimitity for representations of locally compact groups Proc. N.A.S. 35: p.537–545, 1949.

[30] J. Marsden and A. Weinstein. Reduction of symplectic manifolds with symmetry. *Rep. Math. Phys.*, 5:121–130, 1974.

[31] D. Mumford. Elastica and computer vision. *Algebraic Geometry and Its Applications. Springer-Verlag*, pages 491–506, 1994.

[32] M. Nitzberg and T. Shiota. Nonlinear image filtering with edge and corner enhancement. *IEEE Transactions on Pattern Analysis and Machine Intelligence, 14:826–833, 1992.*

[33] P. Perona and J. Malik. Scale-space and edge detection using anisotropic diffusion. *IEEE-transactions on Pattern Analysis and Machine Intelligence*, (7).

[34] H.G.J. Pijls. The Yang-Mills equations. *In proc. seminar 1981-1982 mathematical structures in field theories, ed. E.M. de Jager and H.G.J. Pijls, p.119–182, 1984*

[35] N.A. Sochen. Stochastic Processes in Vision I: From Langevin to Beltrami. Center for Communication and Information Technologies, Department of Electrical Engineering, Technion, Israël Institute of Technology, Haifa 32000, Israël", June 1999, Tech. rep. CC PUB #285.

[36] M. Spivak Differntial geometry Vol II, Publish or Perish inc. 1975.

[37] S. Sternberg. *Lectures on Differntial Geometry*. Prentice Hall Math. Series, Prentice Hall Inc., 1964.

[38] A.F.M. ter Elst and D.W. Robinson Weighted Subcoercive Operators on Lie Groups *Journal of Functional Analysis*, 157:88–163, 1998.

[39] M. Unser. A perfect fit for signal and image processing. *IEEE-signal processing magazine*, pages 27–37, November 1999.

[40] M. van Ginkel Image Analysis using Orientation Space based on Steerable Filters PhD thesis, Delft University of Technology, Department of Biomedical Engineering, Eindhoven the Netherlands, October 2002.

[41] V.S. Varadarajan. *Lie Groups, Lie-Algebras and Their Representations*. Springer-Verlag, New York, Berlin, Heidelberg, Tokyo, 1984.

[42] J. A. Weickert. *Anisotropic Diffusion in Image Processing*. ECMI Series. Teubner, Stuttgart, January 1998.

[43] J. A. Weickert. Coherence-enhancing diffusion filtering. *International Journal of Computer Vision*, 31(2/3):111–127, April 1999.